Searching for possible Ω_c-like molecular states from meson-baryon interaction

Rui Chen,[1,2,3,*] Atsushi Hosaka,[3,†] and Xiang Liu[1,2,‡]

[1]School of Physical Science and Technology, Lanzhou University, Lanzhou 730000, China
[2]Research Center for Hadron and CSR Physics, Lanzhou University and Institute of Modern Physics of CAS, Lanzhou 730000, China
[3]Research Center for Nuclear Physics (RCNP), Osaka University, Ibaraki, Osaka 567-0047, Japan

(Received 21 November 2017; published 16 February 2018)

Stimulated by the recent observation of Ω_c as well as past observations of $P_c(4380)$ and $P_c(4450)$, we perform a coupled-channel analysis of $\Xi_c^*\bar{K}/\Omega_c\eta/\Omega_c^*\eta/\Xi_c\bar{K}^*/\Xi_c'\bar{K}^*/\Omega_c\omega$ systems to search for possible Ω_c-like molecular states by using a one-boson-exchange potential. Our results suggest that there exists a loosely bound molecular state—a $\Xi_c^*\bar{K}/\Omega_c\eta/\Omega_c^*\eta/\Xi_c\bar{K}^*/\Xi_c'\bar{K}^*/\Omega_c\omega$ with $I(J^P) = 0(3/2^-)$—that is mainly composed of the $\Xi_c^*\bar{K}$ system. The two-body strong decay width is also studied, where we find that $\Xi_c'\bar{K}$ is the dominant decay channel.

DOI: 10.1103/PhysRevD.97.036016

I. INTRODUCTION

In the past 14 years, a series of novel phenomena relevant to the XYZ states have been reported with the accumulation of experimental data. These observations provide us with a good chance to identify the exotic configurations (multiquark states, glueball, hybrid) of hadrons (see the reviews [1,2] for more details). In fact, experimental and theoretical studies on exotic states are a good approach to deepen our understanding of the nonperturbative behavior of QCD.

In 2015, $P_c(4380)$ and $P_c(4450)$ were reported by the LHCb Collaboration in the decay $\Lambda_b^0 \to J/\psi p K^-$ [3], which stimulated theorists' enthusiasm to investigate the heavy pentaquarks. As shown in Fig. 1, the masses of $P_c(4380)$ and $P_c(4450)$ are close to the thresholds of a charmed baryon and anticharmed meson pair, and theorists have tried to describe their inner structures using hadronic molecules [4–16]. In particular, $P_c(4380)$ was interpreted as a loose molecular pentaquark made up of $\Sigma_c^*\bar{D}$ with a binding energy of several MeV. Analogously, with a simple replacement of quarks, it is natural to ask whether there exist possible Ω_c-like molecules composed of a charmed-strange baryon and an antistrange meson. In a sense, this study can enhance our understanding of these P_c states.

In fact, studies of the interaction between one hadron and one strange meson have been carried out for several decades. In these works, observations near a pair of hadron thresholds are often explained as possible molecular states, as shown in Table I. Therefore, searching for exotic states from hadron and strange meson interactions is very important, and further exploration of the interaction between a charmed-strange baryon and an antistrange meson is needed.

The LHCb Collaboration announced that five new Ω_c states were observed in the $\Xi_c^+ K^-$ channel [43]. We should emphasize that no resonant-like signals were found in the $\Xi_c^{*+} K^+$ channel, which is to be expected if the observed states are standard three-quark states. As their masses are very close to the threshold of a charmed-strange baryon and antistrange meson pair, molecular pentaquarks have been proposed in Refs. [44–48]. In this paper, a comprehensive investigation of the $\Xi_c^*\bar{K}/\Omega_c\eta/\Omega_c^*\eta/\Xi_c\bar{K}^*/\Xi_c'\bar{K}^*/\Omega_c\omega$ interaction will be adopted, which is also helpful to understand the nature of these new Ω_c states.

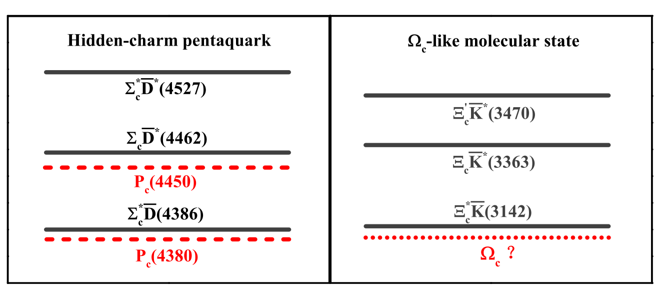

FIG. 1. A comparison of the masses of the heavy pentaquarks and the mass thresholds of antimeson and baryon pair systems.

*chenr15@lzu.edu.cn
†hosaka@rcnp.osaka-u.ac.jp
‡xiangliu@lzu.edu.cn

TABLE I. A summery of the new observations and their corresponding molecular explanations.

Observations	$I(J^P)$	Explanations	Observations	$I(J^P)$	Explanations
$X(5568)$	$1(0^+)$	$B\bar{K}$ [17–23]	$D_{s0}(2317)$	$0(0^+)$	DK [24–29]
$D_{s1}(2460)$	$0(1^+)$	D^*K [29–32]	$f_0(980)$	$0(0^+)$	$K\bar{K}$ [33–35]
$f_1(1285)$	$0(1^+)$	$K^*\bar{K}$ [36–39]	$\Lambda(1405)$	$0(1/2^-)$	$N\bar{K}$ [40–42]

To obtain the effective potential describing the interaction between the charmed-strange baryon and antistrange meson, we adopt the one-boson-exchange (OBE) model—including π, σ, ρ, ω, and ϕ—which is often used to identify and predict exotic states, such as $X/Y/Z/P_c$ states. Both the S-D mixing effect and the coupled-channel effect will also be considered here. This study will provide valuable information to searches for Ω_c-like molecular states composed of a charmed-strange baryon and antistrange meson. What is more important is that it will also provide a test of the molecular-state picture for $P_c(4380)$ and $P_c(4450)$.

This paper is organized as follows. In Sec. II the interaction of a charmed-strange baryon and antistrange meson is studied using the OBE model and the coupled-channel effect. The decay of the possible molecular candidates is further discussed in Sec. III. The paper ends with a discussion and conclusion in Sec. V.

II. THE $\Xi_c^{(\prime,*)}\bar{K}^{(*)}$ INTERACTIONS

A. Lagrangians

Let us start with the effective Lagrangian approach at the hadronic level. If we consider the heavy-quark limit and chiral symmetry [49], the effective Lagrangians relevant to the charmed-strange baryon are

$$\mathcal{L}_{\mathcal{B}_{\bar{3}}} = l_B\langle\bar{\mathcal{B}}_{\bar{3}}\sigma\mathcal{B}_{\bar{3}}\rangle + i\beta_B\langle\bar{\mathcal{B}}_{\bar{3}}v^\mu(\mathcal{V}_\mu-\rho_\mu)\mathcal{B}_{\bar{3}}\rangle, \tag{1}$$

$$\begin{aligned}\mathcal{L}_{\mathcal{B}_6} &= l_S\langle\bar{\mathcal{S}}_\mu\sigma\mathcal{S}^\mu\rangle - \frac{3}{2}g_1\varepsilon^{\mu\nu\lambda\kappa}v_\kappa\langle\bar{\mathcal{S}}_\mu A_\nu\mathcal{S}_\lambda\rangle \\ &\quad + i\beta_S\langle\bar{\mathcal{S}}_\mu v_\alpha(\mathcal{V}^\alpha_{ab}-\rho^\alpha_{ab})\mathcal{S}^\mu\rangle + \lambda_S\langle\bar{\mathcal{S}}_\mu F^{\mu\nu}(\rho)\mathcal{S}_\nu\rangle,\end{aligned} \tag{2}$$

$$\mathcal{L}_{\mathcal{B}_{\bar{3}}\mathcal{B}_6} = ig_4\langle\bar{\mathcal{S}}^\mu A_\mu\mathcal{B}_{\bar{3}}\rangle + i\lambda_I\varepsilon^{\mu\nu\lambda\kappa}v_\mu\langle\bar{\mathcal{S}}_\nu F_{\lambda\kappa}\mathcal{B}_{\bar{3}}\rangle + \text{H.c.} \tag{3}$$

In the above formulas, A_μ and $\mathcal{V}_\mu$ are the axial current and vector current, respectively,

$$\begin{aligned}A_\mu &= \frac{1}{2}(\xi^\dagger\partial_\mu\xi - \xi\partial_\mu\xi^\dagger) = \frac{i}{f_\pi}\partial_\mu P + \cdots, \\ \mathcal{V}_\mu &= \frac{1}{2}(\xi^\dagger\partial_\mu\xi + \xi\partial_\mu\xi^\dagger) = \frac{i}{2f_\pi^2}[P,\partial_\mu P] + \cdots,\end{aligned}$$

where $\xi = \exp(iP/f_\pi)$, the pion decay constant $f_\pi = 132$ MeV, $\rho^\mu_{ba} = ig_V V^\mu_{ba}/\sqrt{2}$, and $F^{\mu\nu}(\rho) = \partial^\mu\rho^\nu - \partial^\nu\rho^\mu + [\rho^\mu,\rho^\nu]$. $\mathcal{S}$ is defined as a superfield, which includes $\mathcal{B}_6$ with $J^P = 1/2^+$ and $\mathcal{B}_6^*$ with $J^P = 3/2^+$ in the 6_F flavor representation, i.e., $\mathcal{S}_\mu = -\sqrt{\frac{1}{3}}(\gamma_\mu + v_\mu)\gamma^5\mathcal{B}_6 + \mathcal{B}^*_{6\mu}$. The matrices $\mathcal{B}_{\bar{3}}$, $\mathcal{B}_6^{(*)}$, P, and V are expressed as

$$\mathcal{B}_{\bar{3}} = \begin{pmatrix} 0 & \Lambda_c^+ & \Xi_c^+ \\ -\Lambda_c^+ & 0 & \Xi_c^0 \\ -\Xi_c^+ & -\Xi_c^0 & 0 \end{pmatrix},$$

$$\mathcal{B}_6^{(*)} = \begin{pmatrix} \Sigma_c^{(*)++} & \frac{\Sigma_c^{(*)+}}{\sqrt{2}} & \frac{\Xi_c^{(\prime,*)+}}{\sqrt{2}} \\ \frac{\Sigma_c^{(*)+}}{\sqrt{2}} & \Sigma_c^{(*)0} & \frac{\Xi_c^{(\prime,*)0}}{\sqrt{2}} \\ \frac{\Xi_c^{(\prime,*)+}}{\sqrt{2}} & \frac{\Xi_c^{(\prime,*)0}}{\sqrt{2}} & \Omega_c^{(*)0} \end{pmatrix},$$

$$P = \begin{pmatrix} \frac{\pi^0}{\sqrt{2}} & \pi^+ & K^+ \\ \pi^- & -\frac{\pi^0}{\sqrt{2}} & K^0 \\ K^- & \bar{K}^0 & -\frac{2}{\sqrt{6}}\eta \end{pmatrix},$$

$$V = \begin{pmatrix} \frac{\rho^0}{\sqrt{2}} + \frac{\omega}{\sqrt{2}} & \rho^+ & K^{*+} \\ \rho^- & -\frac{\rho^0}{\sqrt{2}} + \frac{\omega}{\sqrt{2}} & K^{*0} \\ K^{*-} & \bar{K}^{*0} & \phi \end{pmatrix}.$$

For the strange meson part, the effective Lagrangians are constructed as [50,51]

$$\begin{aligned}\mathcal{L} &= \mathcal{L}_{PPV} + \mathcal{L}_{VVP} + \mathcal{L}_{VVV} \\ &= \frac{ig}{2\sqrt{2}}\langle\partial^\mu P(PV_\mu - V_\mu P)\rangle + \frac{g_{VVP}}{\sqrt{2}}\epsilon^{\mu\nu\alpha\beta}\langle\partial_\mu V_\nu\partial_\alpha V_\beta P\rangle \\ &\quad + \frac{ig}{2\sqrt{2}}\langle\partial^\mu V^\nu(V_\mu V_\nu - V_\nu V_\mu)\rangle.\end{aligned} \tag{4}$$

By expanding Eqs. (1)–(4), one can further obtain

$$\mathcal{L}_{\mathcal{B}_{\bar{3}}\mathcal{B}_{\bar{3}}\sigma} = l_B\langle\bar{\mathcal{B}}_{\bar{3}}\sigma\mathcal{B}_{\bar{3}}\rangle, \tag{5}$$

$$\begin{aligned}\mathcal{L}_{\mathcal{B}_6^{(*)}\mathcal{B}_6^{(*)}\sigma} &= -l_S\langle\bar{\mathcal{B}}_6\sigma\mathcal{B}_6\rangle + l_S\langle\bar{\mathcal{B}}^*_{6\mu}\sigma\mathcal{B}_6^{*\mu}\rangle \\ &\quad - \frac{l_S}{\sqrt{3}}\langle\bar{\mathcal{B}}^*_{6\mu}\sigma(\gamma^\mu + v^\mu)\gamma^5\mathcal{B}_6\rangle + \text{H.c.},\end{aligned} \tag{6}$$

$$\mathcal{L}_{\mathcal{B}_{\bar{3}}\mathcal{B}_{\bar{3}}V} = \frac{1}{\sqrt{2}}\beta_B g_V\langle\bar{\mathcal{B}}_{\bar{3}}v\cdot V\mathcal{B}_{\bar{3}}\rangle, \tag{7}$$

TABLE II. Coupling constants adopted in our calculation [49,50]. $g_{VVP} = 3g^2/(32\sqrt{2}\pi^2 f_\pi)$ [51].

l_B	$\beta_B g_V$	l_S	g_1	$\beta_S g_V$	$\lambda_S g_V$ (GeV^{-1})	g_4	$\lambda_I g_V$ (GeV^{-1})	g_σ	g
−3.65	−6.0	7.3	1.0	12.0	19.2	1.06	−6.8	3.65	12.0

$$\mathcal{L}_{\mathcal{B}_6^{(*)}\mathcal{B}_6^{(*)}P} = i\frac{g_1}{2f_\pi}\varepsilon^{\mu\nu\lambda\kappa}v_\kappa\langle\bar{\mathcal{B}}_6\gamma_\mu\gamma_\lambda\partial_\nu P\mathcal{B}_6\rangle + i\frac{\sqrt{3}}{2}\frac{g_1}{f_\pi}v_\kappa\varepsilon^{\mu\nu\lambda\kappa}\langle\bar{\mathcal{B}}^*_{6\mu}\partial_\nu P\gamma_\lambda\gamma^5\mathcal{B}_6\rangle + \text{H.c.} - i\frac{3g_1}{2f_\pi}\varepsilon^{\mu\nu\lambda\kappa}v_\kappa\langle\bar{\mathcal{B}}^*_{6\mu}\partial_\nu P\mathcal{B}^*_{6\lambda}\rangle, \quad (8)$$

$$\begin{aligned}\mathcal{L}_{\mathcal{B}_6^{(*)}\mathcal{B}_6^{(*)}V} = &-\frac{\beta_S g_V}{\sqrt{2}}\langle\bar{\mathcal{B}}_6 v\cdot V\mathcal{B}_6\rangle - i\frac{\lambda g_V}{3\sqrt{2}}\langle\bar{\mathcal{B}}_6\gamma_\mu\gamma_\nu(\partial^\mu V^\nu - \partial^\nu V^\mu)\mathcal{B}_6\rangle - \frac{\beta_S g_V}{\sqrt{6}}\langle\bar{\mathcal{B}}^*_{6\mu}v\cdot V(\gamma^\mu + v^\mu)\gamma^5\mathcal{B}_6\rangle \\ &- i\frac{\lambda_S g_V}{\sqrt{6}}\langle\bar{\mathcal{B}}^*_{6\mu}(\partial^\mu V^\nu - \partial^\nu V^\mu)(\gamma_\nu + v_\nu)\gamma^5\mathcal{B}_6\rangle + \frac{\beta_S g_V}{\sqrt{2}}\langle\bar{\mathcal{B}}^*_{6\mu}v\cdot V\mathcal{B}_6^{*\mu}\rangle + i\frac{\lambda_S g_V}{\sqrt{2}}\langle\bar{\mathcal{B}}^*_{6\mu}(\partial^\mu V^\nu - \partial^\nu V^\mu)\mathcal{B}^*_{6\nu}\rangle + \text{H.c.}, \quad (9)\end{aligned}$$

$$\mathcal{L}_{\mathcal{B}_{\bar{3}}\mathcal{B}_6^{(*)}V} = -\frac{\lambda_I g_V}{\sqrt{6}}\varepsilon^{\mu\nu\lambda\kappa}v_\mu\langle\bar{\mathcal{B}}_6\gamma^5\gamma_\nu(\partial_\lambda V_\kappa - \partial_\kappa V_\lambda)\mathcal{B}_{\bar{3}}\rangle - \frac{\lambda_I g_V}{\sqrt{2}}\varepsilon^{\mu\nu\lambda\kappa}v_\mu\langle\bar{\mathcal{B}}^*_{6\nu}(\partial_\lambda V_\kappa - \partial_\kappa V_\lambda)\mathcal{B}_{\bar{3}}\rangle + \text{H.c.}, \quad (10)$$

$$\mathcal{L}_{\mathcal{B}_{\bar{3}}\mathcal{B}_6^{(*)}P} = -\sqrt{\frac{1}{3}}\frac{g_4}{f_\pi}\langle\bar{\mathcal{B}}_6\gamma^5(\gamma^\mu + v^\mu)\partial_\mu P\mathcal{B}_{\bar{3}}\rangle - \frac{g_4}{f_\pi}\langle\bar{\mathcal{B}}^*_{6\mu}\partial^\mu P\mathcal{B}_{\bar{3}}\rangle + \text{H.c.}, \quad (11)$$

$$\mathcal{L}_{\pi KK^*} = \frac{ig}{4}[(\bar{K}^{*\mu}\boldsymbol{\tau}\cdot K - \bar{K}\boldsymbol{\tau}\cdot K^{*\mu})\partial_\mu\boldsymbol{\pi} + (\partial_\mu\bar{K}\boldsymbol{\tau}\cdot K^{*\mu} - \bar{K}^{*\mu}\boldsymbol{\tau}\cdot\partial_\mu K)\boldsymbol{\pi}], \quad (12)$$

$$\mathcal{L}_{\mathbb{V}KK} = \frac{ig}{4}[\bar{K}(\boldsymbol{\tau}\cdot\boldsymbol{\rho}^\mu + \omega^\mu - \sqrt{2}\phi^\mu)\partial_\mu K - \partial_\mu\bar{K}(\boldsymbol{\tau}\cdot\boldsymbol{\rho}^\mu + \omega^\mu - \sqrt{2}\phi^\mu)K], \quad (13)$$

$$\begin{aligned}\mathcal{L}_{\mathbb{V}K^*K^*} = \frac{ig}{4}[&(\bar{K}^*_\mu\partial^\mu K^{*\nu} - \partial^\mu\bar{K}^{*\nu}K^*_\mu)(\boldsymbol{\tau}\cdot\boldsymbol{\rho}_\nu + \omega_\nu - \sqrt{2}\phi_\nu) + (\partial^\mu\bar{K}^{*\nu}K^*_\nu - \bar{K}^*_\nu\partial^\mu K^{*\nu})(\boldsymbol{\tau}\cdot\boldsymbol{\rho}_\mu + \omega_\mu - \sqrt{2}\phi_\mu) \\ &+ (\bar{K}^*_\nu K^*_\mu - \bar{K}^*_\mu K^*_\nu)(\boldsymbol{\tau}\cdot\partial^\mu\boldsymbol{\rho}^\nu + \partial^\mu\omega^\nu - \sqrt{2}\partial^\mu\phi^\nu)], \quad (14)\end{aligned}$$

$$\mathcal{L}_{\pi K^*K^*} = g_{VVP}\varepsilon_{\mu\nu\alpha\beta}\partial^\mu\bar{K}^{*\nu}\partial^\alpha K^{*\beta}\boldsymbol{\tau}\cdot\boldsymbol{\pi}, \quad (15)$$

$$\mathcal{L}_{\mathbb{V}KK^*} = g_{VVP}\varepsilon_{\mu\nu\alpha\beta}(\partial^\mu\bar{K}^{*\nu}K + \bar{K}\partial^\mu K^{*\nu})(\boldsymbol{\tau}\cdot\partial^\alpha\boldsymbol{\rho}^\beta + \partial^\alpha\omega^\beta - \sqrt{2}\partial^\alpha\phi^\beta). \quad (16)$$

Here, $\boldsymbol{\tau}$ is Pauli matrix, and $\boldsymbol{\pi}$ and $\boldsymbol{\rho}$ denote the pion and rho meson isospin triplets, respectively. For the σ-exchange vertex, we use

$$\mathcal{L}_{\sigma K^{(*)}K^{(*)}} = g_\sigma\bar{K}K\sigma + g_\sigma\bar{K}^{*\mu}K^*_\mu\sigma. \quad (17)$$

The coupling constants in the above Lagrangians are collected in Table II. The corresponding phase factors between these coupling constants are determined by the quark model.

By adopting the Breit approximation, the effective potentials can be related to the scattering amplitudes by

$$\mathcal{V}_E^{h_1h_2\to h_3h_4}(\boldsymbol{q}) = -\frac{\mathcal{M}(h_1h_2\to h_3h_4)}{\sqrt{\prod_i 2M_i\prod_f 2M_f}}. \quad (18)$$

For the scattering process $h_1h_2\to h_3h_4$, M_i and M_f are the masses of the initial states (h_1, h_2) and final states (h_3, h_4), respectively. $\mathcal{M}(h_1h_2\to h_3h_4)$ denotes the scattering amplitude for the $h_1h_2\to h_3h_4$ process by exchanging one boson (σ, π, ρ, ω, and ϕ) in the t channel. The effective potential in the coordinate space $\mathcal{V}(\boldsymbol{r})$ can be obtained by performing a Fourier transformation, i.e.,

$$\mathcal{V}_E^{h_1h_2\to h_3h_4}(\boldsymbol{r}) = \int\frac{d^3\boldsymbol{q}}{(2\pi)^3}e^{i\boldsymbol{q}\cdot\boldsymbol{r}}\mathcal{V}_E^{h_1h_2\to h_3h_4}(\boldsymbol{q})\mathcal{F}^2(q^2, m_E^2).$$

In the above equation, a monopole form factor $\mathcal{F}(q^2, m_E^2) = (\Lambda^2 - m_E^2)/(\Lambda^2 - q^2)$ is introduced at every interactive vertex to express the off-shell effect of the exchanged boson, where Λ, m_E, and q are the cutoff, mass, and four-momentum of the exchanged meson, respectively.

B. A single-channel analysis

In this subsection, we discuss the single $\Xi_c^*\bar{K}$ system before performing our full coupled-channel study. This is a

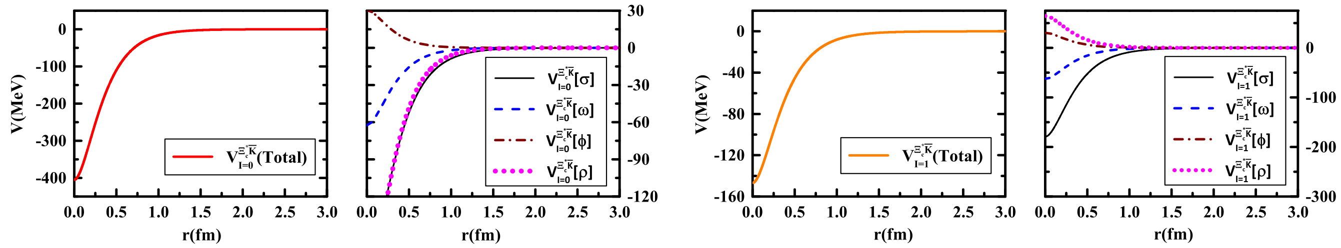

FIG. 2. r dependence of the deduced effective potentials with the cutoff $\Lambda = 1.25$ GeV for the $\Xi_c^*\bar{K}$ system.

useful way to indicate the importance of the coupled channels of $\Xi_c^*\bar{K}/\Xi_c\bar{K}^*/\Xi_c'\bar{K}^*$. The OBE effective potential for the S-wave $\Xi_c^*\bar{K}$ system is given as

$$\mathcal{V}_I^{\Xi_c^*\bar{K}}(r) = -\frac{1}{2}l_S g_\sigma Y(\Lambda, m_\sigma, r) - \frac{1}{16}\beta_S g_V g[\mathcal{G}(I)Y(\Lambda, m_\rho, r) + Y(\Lambda, m_\omega, r) - 2Y(\Lambda, m_\phi, r)], \tag{19}$$

where $\mathcal{G}(I)$ is the isospin factor, which is 3 for the isoscalar system and -1 for the isovector system. The corresponding flavor wave functions $|I, I_3\rangle$ for the $\Xi_c^*\bar{K}$ system are $|0,0\rangle = (|\Xi_c^{*+}K^-\rangle + |\Xi_c^{*0}\bar{K}^0\rangle)/\sqrt{2}$, $|1,1\rangle = |\Xi_c^{*+}\bar{K}^0\rangle$, $|1,-1\rangle = |\Xi_c^{*0}K^-\rangle$, and $|1,0\rangle = (|\Xi_c^{*+}K^-\rangle - |\Xi_c^{*0}\bar{K}^0\rangle)/\sqrt{2}$, respectively. In addition, the function $Y(\Lambda, m, r)$ denotes

$$Y(\Lambda, m, r) = \frac{1}{4\pi r}(e^{-mr} - e^{-\Lambda r}) - \frac{\Lambda^2 - m^2}{8\pi\Lambda}e^{-\Lambda r}. \tag{20}$$

Here the cutoff Λ is a parameter of the OBE potential. As is well known, reasonable values of the cutoff are around $\Lambda \sim 1$ GeV [52,53], corresponding to the typical hadronic scale or the intrinsic size of hadrons. As we will see in the following sections, in the present paper we attempt to find bound-state solutions by varying the cutoff parameter to obtain a binding energy around a few to 10 MeV for loosely bound molecular hadrons. The physical relevance of the results will be discussed in terms of the cutoff parameters.

In Fig. 2, we present the r dependence of the effective potentials for the $\Xi_c^*\bar{K}$ system with $I = 0, 1$, and its cutoff Λ is taken as 1.25 GeV.

According to the effective potential in Fig. 2, we can make the following summary.

(1) There is no π-exchange contribution, as the spin-parity conservation forbids the vertex $\bar{K} - \bar{K} - \pi$.

(2) The interactions from σ exchange are attractive and dominant, which is consistent with the conclusions in Ref. [54].

(3) As discussed in Ref. [54], the interaction of ω exchange is different for a hadron-hadron system with light quark-quark or quark-antiquark combinations. For the $\Xi_c^*\bar{K}$ system, its quark configuration is $(csq) - (s\bar{q})$. The ω exchange from the combination of $q - \bar{q}$ provides an attractive interaction.

(4) In comparison with the ω exchange, the ϕ meson couples to the strange quark(s) and/or antistrange quark(s). Here, the $s - \bar{s}$ combination from the $\Xi_c^*\bar{K}$ system implies that the interaction from the ϕ exchange is repulsive.

(5) The ρ meson couples to the isospin charge, and thus in the isoscalar $\Xi_c^*\bar{K}$ system the interaction from ρ exchange is attractive and almost 3 times stronger than that in the isovector $\Xi_c^*\bar{K}$ system.

By adopting the effective potential in Eq. (19), we numerically solve the Schrödinger equation, with the cutoff Λ being scanned from 1 to 5 GeV. Finally, only the $\Xi_c^*\bar{K}$ state with $[I(J^P) = 0(3/2^-)]$ can generate bound solutions when Λ is taken larger than 1.60 GeV. As the cutoff Λ is increased, it binds more strongly. In particular, when Λ is fixed at 2.30 GeV, its binding energy reaches -21.15 MeV. Then, the mass of the $\Xi_c^*\bar{K}$ state with $I(J^P) = 0(3/2^-)$ is close to the observed mass of the newly reported $\Omega_c(3119)$ in Ref. [43]. However, if we take the cutoff value $\Lambda \sim 1$ GeV [52,53] as a typical hadron scale (which is more reasonable than $\Lambda \sim 2$ GeV), our results indicate there are no bound solutions for the S-wave $\Xi_c^*\bar{K}$ system, although the total OBE effective potential is attractive. For higher partial waves, due to the repulsive centrifugal potential, it is not likely that bound states exist.

To summarize, for the single $\Xi_c^*\bar{K}$ system, the intermediate-range and short-range forces from the OBE model are not strong enough to generate bound molecular states. Therefore, the new $\Omega_c(3119)$ cannot be a pure $\Xi_c^*\bar{K}$ molecular state. In Ref. [48], the authors proposed that the new $\Omega_c(3119)$ can be associated with a meson-baryon state strongly coupled to $\Xi_c^*\bar{K}$ and $\Omega_c^*\eta$ with $J^P = 3/2^-$ by using the vector-meson exchange interaction in the local hidden gauge method. We find that the vector-exchange model provides an attractive interaction, and the coupled-channel effect is very important, which is also consistent with our present results: considering only the single $\Xi_c^*\bar{K}$ system with the vector-exchange model cannot reproduce the $\Omega_c(3119)$. Thus, in the next section, we will adopt the coupled-channel approach to continue our study. In our present study, we take into account the long-range force from pion exchange, the tensor force, and S-D wave mixing, which we believe are important and were not considered in Ref. [48].

C. $\Xi_c^*\bar{K}/\Omega_c\eta/\Omega_c^*\eta/\Xi_c\bar{K}^*/\Xi_c'\bar{K}^*/\Omega_c\omega$ coupled-channel system

In this section, we consider coupled-channel studies that include the one-pion exchange interaction, as expected

TABLE III. Possible channels involved in our calculation. Here, the first column contains the spin-parity quantum numbers corresponding to the channels.

J^P	Channels					
$1/2^-$	$\Xi_c^*\bar{K}:\vert{}^4\mathbb{D}_{\frac{1}{2}}\rangle$	$\Omega_c\eta:\vert{}^2\mathbb{S}_{\frac{1}{2}}\rangle$	$\Omega_c^*\eta:\vert{}^4\mathbb{D}_{\frac{1}{2}}\rangle$	$\Xi_c\bar{K}^*:\vert{}^2\mathbb{S}_{\frac{1}{2}}/{}^4\mathbb{D}_{\frac{1}{2}}\rangle$	$\Xi_c'\bar{K}^*:\vert{}^2\mathbb{S}_{\frac{1}{2}}/{}^4\mathbb{D}_{\frac{1}{2}}\rangle$	$\Omega_c\omega:\vert{}^2\mathbb{S}_{\frac{1}{2}}/{}^4\mathbb{D}_{\frac{1}{2}}\rangle$
$3/2^-$	$\Xi_c^*\bar{K}:\vert{}^4\mathbb{S}_{\frac{3}{2}}/{}^4\mathbb{D}_{\frac{3}{2}}\rangle$	$\Omega_c\eta:\vert{}^2\mathbb{D}_{\frac{3}{2}}\rangle$	$\Omega_c^*\eta:\vert{}^4\mathbb{S}_{\frac{3}{2}}/{}^4\mathbb{D}_{\frac{3}{2}}\rangle$	$\Xi_c\bar{K}^*:\vert{}^4\mathbb{S}_{\frac{3}{2}}/{}^2\mathbb{D}_{\frac{3}{2}}/{}^4\mathbb{D}_{\frac{3}{2}}\rangle$	$\Xi_c'\bar{K}^*:\vert{}^4\mathbb{S}_{\frac{3}{2}}/{}^2\mathbb{D}_{\frac{3}{2}}/{}^4\mathbb{D}_{\frac{3}{2}}\rangle$	$\Omega_c\omega:\vert{}^4\mathbb{S}_{\frac{3}{2}}/{}^2\mathbb{D}_{\frac{3}{2}}/{}^4\mathbb{D}_{\frac{3}{2}}\rangle$
$5/2^-$	$\Xi_c^*\bar{K}:\vert{}^4\mathbb{D}_{\frac{5}{2}}\rangle$	$\Omega_c\eta:\vert{}^2\mathbb{D}_{\frac{5}{2}}\rangle$	$\Omega_c^*\eta:\vert{}^4\mathbb{D}_{\frac{5}{2}}\rangle$	$\Xi_c\bar{K}^*:\vert{}^2\mathbb{D}_{\frac{5}{2}}/{}^4\mathbb{D}_{\frac{5}{2}}\rangle$	$\Xi_c'\bar{K}^*:\vert{}^2\mathbb{D}_{\frac{5}{2}}/{}^4\mathbb{D}_{\frac{5}{2}}\rangle$	$\Omega_c\omega:\vert{}^2\mathbb{D}_{\frac{5}{2}}/{}^4\mathbb{D}_{\frac{5}{2}}\rangle$
$1/2^+$	$\Xi_c^*\bar{K}:\vert{}^4\mathbb{P}_{\frac{1}{2}}\rangle$	$\Omega_c\eta:\vert{}^2\mathbb{P}_{\frac{1}{2}}\rangle$	$\Omega_c^*\eta:\vert{}^4\mathbb{P}_{\frac{1}{2}}\rangle$	$\Xi_c\bar{K}^*:\vert{}^2\mathbb{P}_{\frac{1}{2}}/{}^4\mathbb{P}_{\frac{1}{2}}\rangle$	$\Xi_c'\bar{K}^*:\vert{}^2\mathbb{P}_{\frac{1}{2}}/{}^4\mathbb{P}_{\frac{1}{2}}\rangle$	$\Omega_c\omega:\vert{}^2\mathbb{P}_{\frac{1}{2}}/{}^4\mathbb{P}_{\frac{1}{2}}\rangle$
$3/2^+$	$\Xi_c^*\bar{K}:\vert{}^4\mathbb{P}_{\frac{3}{2}}\rangle$	$\Omega_c\eta:\vert{}^2\mathbb{P}_{\frac{3}{2}}\rangle$	$\Omega_c^*\eta:\vert{}^4\mathbb{P}_{\frac{3}{2}}\rangle$	$\Xi_c\bar{K}^*:\vert{}^2\mathbb{P}_{\frac{3}{2}}/{}^4\mathbb{P}_{\frac{3}{2}}\rangle$	$\Xi_c'\bar{K}^*:\vert{}^2\mathbb{P}_{\frac{3}{2}}/{}^4\mathbb{P}_{\frac{3}{2}}\rangle$	$\Omega_c\omega:\vert{}^2\mathbb{P}_{\frac{3}{2}}/{}^4\mathbb{P}_{\frac{3}{2}}\rangle$
$5/2^+$	$\Xi_c^*\bar{K}:\vert{}^4\mathbb{P}_{\frac{5}{2}}\rangle$	$\Omega_c^*\eta:\vert{}^4\mathbb{P}_{\frac{5}{2}}\rangle$	$\Xi_c\bar{K}^*:\vert{}^4\mathbb{P}_{\frac{5}{2}}\rangle$	$\Xi_c'\bar{K}^*:\vert{}^4\mathbb{P}_{\frac{5}{2}}\rangle$	$\Omega_c\omega:\vert{}^4\mathbb{P}_{\frac{5}{2}}\rangle$	

from the nucleon-nucleon interaction. We include the three channels $\Xi_c^*\bar{K}/\Omega_c\eta/\Omega_c^*\eta/\Xi_c\bar{K}^*/\Xi_c'\bar{K}^*/\Omega_c\omega$, and possible quantum numbers are summarized in Table III.

The general expressions for the spin-orbit wave functions $|{}^{2S+1}L_J\rangle$ for the investigated systems are constructed as

$$\Omega_c\eta:|{}^{2S+1}L_J\rangle = \sum_{m_S,m_L} C^{J,M}_{\frac{1}{2}m_S,Lm_L}\chi_{\frac{1}{2}m}|Y_{L,m_L}\rangle,$$

$$\Xi_c^*\bar{K}/\Omega_c^*\eta:|{}^{2S+1}L_J\rangle = \sum_{m_S,m_L} C^{J,M}_{\frac{3}{2}m_S,Lm_L}\Phi_{\frac{3}{2}m_S}|Y_{L,m_L}\rangle,$$

$$\Xi_c^{(\prime)}\bar{K}^*/\Omega_c\omega:|{}^{2S+1}L_J\rangle = \sum_{m,m'}^{m_S,m_L} C^{S,m_S}_{\frac{1}{2}m,1m'}C^{J,M}_{Sm_S,Lm_L}\chi_{\frac{1}{2}m}\epsilon^{m'}|Y_{L,m_L}\rangle.$$

Here, $C^{J,M}_{Sm_S,Lm_L}$, $C^{S,m_S}_{\frac{1}{2}m,1m'}$, and $C^{S,m_S}_{\frac{3}{2}m,1m'}$ are the Clebsch-Gordan coefficients. $\chi_{\frac{1}{2}m}$ and Y_{L,m_L} stand for the spin wave function and the spherical harmonics function, respectively. The polarization vector ϵ for the vector meson is defined as $\epsilon^m_\pm = \mp\frac{1}{\sqrt{2}}(\epsilon^m_x \pm i\epsilon^m_y)$ and $\epsilon^m_0 = \epsilon^m_z$, which satisfy $\epsilon_{\pm1} = \frac{1}{\sqrt{2}}(0,\pm1,i,0)$ and $\epsilon_0 = (0,0,0,-1)$. The polarization tensor $\Phi_{\frac{3}{2}m}$ for the baryon Ξ_c^* with spin 3/2 is constructed as $\Phi_{\frac{3}{2}m} = \sum_{m_1,m_2}\langle\frac{1}{2},m_1;1,m_2|\frac{3}{2},m\rangle\chi_{\frac{1}{2},m_1}\epsilon^{m_2}$.

The total effective potential for the $\Xi_c^*\bar{K}/\Omega_c\eta/\Omega_c^*\eta/\Xi_c\bar{K}^*/\Xi_c'\bar{K}^*/\Omega_c\omega$ system is given in matrix form,

$$\mathcal{V}_{I,J^P} = \begin{pmatrix}
\mathcal{V}^{\Xi_c^*\bar{K}\to\Xi_c^*\bar{K}}_{I,J^P} & \mathcal{V}^{\Omega_c\eta\to\Xi_c^*\bar{K}}_{I,J^P} & \mathcal{V}^{\Omega_c^*\eta\to\Xi_c^*\bar{K}}_{I,J^P} & \mathcal{V}^{\Xi_c\bar{K}^*\to\Xi_c^*\bar{K}}_{I,J^P} & \mathcal{V}^{\Xi_c'\bar{K}^*\to\Xi_c^*\bar{K}}_{I,J^P} & \mathcal{V}^{\Omega_c\omega\to\Xi_c^*\bar{K}}_{I,J^P} \\
\mathcal{V}^{\Xi_c^*\bar{K}\to\Omega_c\eta}_{I,J^P} & \mathcal{V}^{\Omega_c\eta\to\Omega_c\eta}_{I,J^P} & \mathcal{V}^{\Omega_c^*\eta\to\Omega_c\eta}_{I,J^P} & \mathcal{V}^{\Xi_c\bar{K}^*\to\Omega_c\eta}_{I,J^P} & \mathcal{V}^{\Xi_c'\bar{K}^*\to\Omega_c\eta}_{I,J^P} & \mathcal{V}^{\Omega_c\omega\to\Omega_c\eta}_{I,J^P} \\
\mathcal{V}^{\Xi_c^*\bar{K}\to\Omega_c^*\eta}_{I,J^P} & \mathcal{V}^{\Omega_c\eta\to\Omega_c^*\eta}_{I,J^P} & \mathcal{V}^{\Omega_c^*\eta\to\Omega_c^*\eta}_{I,J^P} & \mathcal{V}^{\Xi_c\bar{K}^*\to\Omega_c^*\eta}_{I,J^P} & \mathcal{V}^{\Xi_c'\bar{K}^*\to\Omega_c^*\eta}_{I,J^P} & \mathcal{V}^{\Omega_c\omega\to\Omega_c^*\eta}_{I,J^P} \\
\mathcal{V}^{\Xi_c^*\bar{K}\to\Xi_c\bar{K}^*}_{I,J^P} & \mathcal{V}^{\Omega_c\eta\to\Xi_c\bar{K}^*}_{I,J^P} & \mathcal{V}^{\Omega_c^*\eta\to\Xi_c\bar{K}^*}_{I,J^P} & \mathcal{V}^{\Xi_c\bar{K}^*\to\Xi_c\bar{K}^*}_{I,J^P} & \mathcal{V}^{\Xi_c'\bar{K}^*\to\Xi_c\bar{K}^*}_{I,J^P} & \mathcal{V}^{\Omega_c\omega\to\Xi_c\bar{K}^*}_{I,J^P} \\
\mathcal{V}^{\Xi_c^*\bar{K}\to\Xi_c'\bar{K}^*}_{I,J^P} & \mathcal{V}^{\Omega_c\eta\to\Xi_c'\bar{K}^*}_{I,J^P} & \mathcal{V}^{\Omega_c^*\eta\to\Xi_c'\bar{K}^*}_{I,J^P} & \mathcal{V}^{\Xi_c\bar{K}^*\to\Xi_c'\bar{K}^*}_{I,J^P} & \mathcal{V}^{\Xi_c'\bar{K}^*\to\Xi_c'\bar{K}^*}_{I,J^P} & \mathcal{V}^{\Omega_c\omega\to\Xi_c'\bar{K}^*}_{I,J^P} \\
\mathcal{V}^{\Xi_c^*\bar{K}\to\Omega_c\omega}_{I,J^P} & \mathcal{V}^{\Omega_c\eta\to\Omega_c\omega}_{I,J^P} & \mathcal{V}^{\Omega_c^*\eta\to\Omega_c\omega}_{I,J^P} & \mathcal{V}^{\Xi_c\bar{K}^*\to\Omega_c\omega}_{I,J^P} & \mathcal{V}^{\Xi_c'\bar{K}^*\to\Omega_c\omega}_{I,J^P} & \mathcal{V}^{\Omega_c\omega\to\Omega_c\omega}_{I,J^P}
\end{pmatrix}, \quad (21)$$

where the subscripts I and J^P represent the isospin and spin-parity of the $\Xi_c^*\bar{K}/\Omega_c\eta/\Omega_c^*\eta/\Xi_c\bar{K}^*/\Xi_c'\bar{K}^*/\Omega_c\omega$ system, respectively. The superscript stands for the corresponding scattering process. The exact expressions for each component shown in Eq. (21) are presented in the Appendix.

Now that we have prepared the effective potentials, in the following we will solve the coupled Schrödinger equation to search for bound states, where the cutoff Λ is scanned from 1 to 5 GeV. Before we show our numerical results, several remarks are in order regarding the relation between a loosely bound molecular scenario and the cutoff parameter Λ introduced in the form factor.

(1) For a molecular state composed of hadrons A and B, its mass is determined as $M = M_A + M_B + E$, where E is the binding energy. For large r where the interaction is sufficiently suppressed, the asymptotic form of the wave function for the S-wave AB molecular state has the form $\psi(r) \sim e^{-\sqrt{2\mu E}r}/r$, where $\mu = M_A M_B/(M_A + M_B)$ is the reduced mass. By using the approximate wave function, we find the relation between the size and the binding energy of the molecular state, $R \sim 1/\sqrt{2\mu E}$. For a loosely bound state, the size of the system should be much larger than the size of all component hadrons, say, a

few fm or larger. Therefore, a good candidate for molecular states should have a binding energy around several MeV or less.

(2) In the coupled-channel approach, the binding energy E is measured from the lowest mass threshold $M_{\rm th}$ among various channels. Here, we introduce another energy $\tilde{E}$ measured from the mass threshold of the most dominant channel $M_{\rm dom}$, $\tilde{E}=E+(M_{\rm th}-M_{\rm dom})$. For example, if there is a bound state for the $\Xi_c^*\bar{K}/\Xi_c\bar{K}^*/\Xi_c'\bar{K}^*$ system, and $\Xi_c'\bar{K}^*$ is the dominant channel, $\tilde{E}=E+(M_{\Xi_c^*\bar{K}}-M_{\Xi_c'\bar{K}^*})$, which may amount to several hundreds of MeV. If $\tilde{E}\sim 200$ MeV, by using the relation $R\sim 1/\sqrt{2\mu E_{bin}}$, we find that the size R turns out to be about 0.5 fm or even less, which cannot be identified with a molecular state.

(3) Because the hadrons are not pointlike particles, we introduce a form factor in a monopole manner at every interaction vertex. For a typical hadronic scale [52,53], a reasonable value of the cutoff Λ should be around 1 GeV.

According to the above discussions, in Table IV we show the results for the binding energies, root-mean-square radii $r_{\rm rms}$, and probabilities of various components of wave functions for all possible spin-parity configurations. There, the binding energies are measured from the lowest threshold, for which we show the results around a few MeV by tuning the cutoff Λ to respect the criterion for the molecular state. For each case, we show the results for three different Λ values to show any possible Λ dependence. From the numerical results presented in Table IV, we see the following.

(1) For $I(J^P)=0(3/2^-)$, when the cutoff Λ is taken around 1.30 GeV, there is one bound state solution with a binding energy of several MeV and a rms radius larger than 1 fm. Compared to the results for the deuteron [52,53], the $\Xi_c^*\bar{K}/\Xi_c\bar{K}^*/\Xi_c'\bar{K}^*$ state with $I(J^P)=0(3/2^-)$ is a candidate for a molecular state. In this state, the $\Xi_c^*\bar{K}|^4S_{\frac{3}{2}}\rangle$ channel has the dominant contribution, which is more than 50% for the $\Xi_c^*\bar{K}/\Omega_c\eta/\Omega_c^*\eta/\Xi_c\bar{K}^*/\Xi_c'\bar{K}^*/\Omega_c\omega$ molecular state. Since this state satisfies the requirements for a loosely bound system (with a size of a few fm and a cutoff around 1 GeV), it is a good candidate for a hadronic molecule with the quantum numbers of Ω_c.

(2) For $I(J^P)=0(1/2^-)$, it is possible to find a bound state with a binding energy around a few MeV with the cutoff Λ around 1 GeV. However, the resulting bound states have small sizes as their corresponding rms radii are around 0.5 fm. We shall come back to this point shortly.

(3) For $I(J^P)=0(3/2^+)$, when the cutoff Λ is around 2 GeV, a loosely bound solution is obtained and its rms radius is around 1 fm with a binding energy of several MeV. The $\Xi_c^*\bar{K}$ and $\Xi_c\bar{K}^*$ systems are the dominant channels. If a cutoff value around 2 GeV is a reasonable input, we may conclude that a loosely bound state exists.

(4) For $I(J^P)=0(1/2^+)$ and $0(5/2^+)$, bound state solutions can also be obtained by choosing the cutoff Λ around 2 GeV or even larger. Moreover, the resulting sizes are too small—around 0.5 fm or less.

(5) For $I(J^P)=0(5/2^-)$, as its cutoff Λ is far away from 1 GeV, it is not a reasonable molecular candidate.

A possible reason for too small sizes for $I(J^P)=0(1/2^\pm,5/2^\pm)$ $\Xi_c^*\bar{K}/\Omega_c\eta/\Omega_c^*\eta/\Xi_c\bar{K}^*/\Xi_c'\bar{K}^*/\Omega_c\omega$ states is that

TABLE IV. Bound-state properties (binding energy E and root-mean-square radius $r_{\rm rms}$) for all of the investigated systems after the coupled-channel effects are considered. The probabilities for the different channels are also given. E, $r_{\rm rms}$, and Λ are in units of MeV, fm, and GeV, respectively. To emphasize the dominant channel, we label the probability for the corresponding channel in bold.

$I(J^P)$	Λ	E	$r_{\rm rms}$	$\Xi_c^*\bar{K}(\%)$	$\Omega_c\eta(\%)$	$\Omega_c^*\eta(\%)$	$\Xi_c\bar{K}^*(\%)$	$\Xi_c'\bar{K}^*(\%)$	$\Omega_c\omega(\%)$
$0(1/2^-)$	1.182	−0.53	0.74	15.97	0.63	0.75	**70.21**	11.98	6.03
	1.186	−3.28	0.71	15.63	0.65	0.75	**70.46**	12.06	6.06
	1.190	−6.06	0.69	15.34	0.66	0.76	**70.67**	12.12	6.10
$0(1/2^+)$	1.709	−0.26	0.59	1.85	0.28	0.19	**52.85**	18.66	26.22
	1.712	−4.18	0.50	1.16	0.28	0.16	**55.00**	18.94	26.15
	1.715	−8.15	0.48	0.84	0.28	0.14	**53.03**	19.11	26.59
$0(3/2^-)$	1.270	−0.58	5.17	**98.22**	∼0	0.21	1.50	∼0	0.07
	1.320	−6.00	2.17	**92.04**	∼0	0.99	6.68	0.03	0.24
	1.370	−20.55	1.19	**79.27**	∼0	2.48	27.44	0.21	0.50
$0(3/2^+)$	1.945	−0.16	1.44	**38.93**	0.01	6.57	**36.92**	14.63	2.84
	1.949	−3.23	0.95	**36.12**	0.01	6.90	**38.59**	15.39	2.99
	1.953	−6.44	0.81	**34.58**	0.01	7.09	**39.39**	15.85	3.07
$0(5/2^-)$	4.480	−1.98	0.26	6.86	0.09	4.84	**31.52**	**29.67**	**27.01**
	4.482	−6.07	0.26	6.88	0.09	4.86	**31.54**	**29.68**	**26.94**
	4.484	−10.19	0.26	6.90	0.09	4.88	**36.79**	**29.69**	**26.87**
$0(5/2^+)$	2.096	−0.63	0.73	17.94	…	0.48	**45.32**	26.75	9.50
	2.100	−3.47	0.58	17.31	…	0.49	**45.80**	26.82	9.58
	2.104	−6.35	0.53	16.99	…	0.50	**46.10**	26.78	9.63

they are dominated by higher-mass channels, such as $\Xi_c K^*$ and/or $\Xi_c' K^*$. Measuring the binding energies of theses states from the higher mass thresholds, they turn out to be around a few hundred MeV, which explains the small size of the bound state of the higher channels.

According to the above analysis, we have seen that there is one candidate for a molecular-like state in the present approach, $\Xi_c^*\bar{K}/\Omega_c\eta/\Omega_c^*\eta/\Xi_c\bar{K}^*/\Xi_c'\bar{K}^*/\Omega_c\omega$ with $I(J^P)=0(3/2^-)$, which is dominated by $\Xi_c^*\bar{K}$. In comparison with the analysis of a single $\Xi_c^*\bar{K}$ channel (which does not accommodate a bound state solution with a cutoff $\Lambda\sim 1$ GeV), it is implied that the coupled-channel effect is very important in the $\Xi_c^*\bar{K}/\Omega_c\eta/\Omega_c^*\eta/\Xi_c\bar{K}^*/\Xi_c'\bar{K}^*/\Omega_c\omega$ interaction.

Besides the loose molecular state composed of the lowest channel, $\Xi_c^*\bar{K}$, we also obtain several bound solutions, where the dominant channels are the $\Xi_c\bar{K}^*$ and/or $\Xi_c'\bar{K}^*$ channels. Their binding energies measured from these higher-mass thresholds $\tilde{E}$ reach several hundreds of MeV, implying that the relevant OBE interaction is strongly attractive. In many of these cases, however, the cutoff Λ is much larger than 1 GeV. By decreasing Λ the interaction can be weakened, and these tightly bound states of the higher-mass channels may become looser. As a result, they may appear as Feschbach-type resonances. This is an interesting issue, which we leave to a future study.

III. DECAY BEHAVIOR FOR THE PREDICTED Ω_c STATE

In this section, we will discuss the two-body strong decay behaviors for the $\Xi_c^*\bar{K}/\Omega_c\eta/\Omega_c^*\eta/\Xi_c\bar{K}^*/\Xi_c'\bar{K}^*/\Omega_c\omega$ state with $I(J^P)=0(3/2^-)$. A relevant diagram is presented in the left panel of Fig. 3.

In the rest frame of the molecular state MS with mass m_{MS}, its two-body decay width for $MS\to C+D$ is

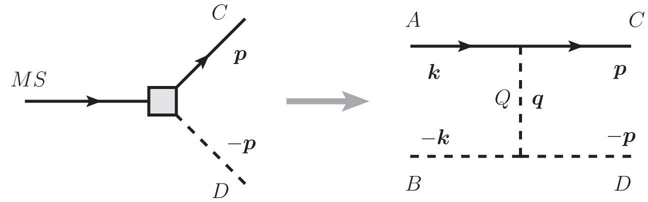

FIG. 3. Left: Two-body strong decay diagram for a molecular state MS into a baryon C and a meson D. Right: MS is composed of two colorless hadrons: a baryon A and a meson B. Q corresponds to the exchanged hadron.

$$d\Gamma=\frac{1}{2J+1}\frac{m_C|\boldsymbol{p}_C|}{8\pi^2 m_{MS}}|\mathcal{M}_I(MS\to C+D)|^2 d\Omega, \quad (22)$$

$$|\boldsymbol{p}_C|=|\boldsymbol{p}_D|=\frac{1}{2m_{MS}}[(m_{MS}^2-(m_C+m_D)^2)\times(m_{MS}^2-(m_C-m_D)^2)]^{1/2}, \quad (23)$$

where particles C and D are the final fermion and boson, respectively.

In Fig. 3, the scattering amplitude for the process $MS\to C+D$ is related to that for the process $A+B\to C+D$,

$$\mathcal{M}_I(MS\to C+D)=\int d^3r\frac{d^3k}{(2\pi)^3}e^{-ik\cdot r}\psi(\boldsymbol{r})\frac{\mathcal{M}_I(A+B\to C+D)}{\sqrt{64m_A m_c m_{MS}}}, \quad (24)$$

where I stands for the isospin of the MS state, and $\psi(\boldsymbol{r})$ is the wave function for the obtained Ω_c state, which was obtained in the last section.

The allowed two-body decay channels for the $\Xi_c^*\bar{K}/\Omega_c\eta/\Omega_c^*\eta/\Xi_c\bar{K}^*/\Xi_c'\bar{K}^*/\Omega_c\omega$ state with $I(J^P)=0(3/2^-)$ include $\Xi_c\bar{K}$ and $\Xi_c'\bar{K}$. The relevant scattering amplitudes are written as

$$\mathcal{M}_I^{(K^*)}(\Omega_c\eta\to\Xi_c\bar{K})=i\frac{\lambda_I g_V}{\sqrt{6}}(\varepsilon^{\mu\nu\lambda\kappa}-\varepsilon^{\mu\nu\kappa\lambda})v_\mu\bar{u}_C\gamma^5\gamma_\nu q_\lambda u_A\frac{g_{\kappa\beta}-q_\kappa q_\beta/m_V^2}{q^2-m_V^2}\frac{g}{4}(P_{B\beta}+P_{D\beta}), \quad (25)$$

$$\mathcal{M}_I^{(K^*)}(\Omega_c\eta\to\Xi_c'\bar{K})=\left(\frac{\beta_S g_V}{\sqrt{2}}\bar{u}_C u_A v_\nu-\frac{\lambda_S g_V}{3\sqrt{2}}\bar{u}_C(\gamma_\mu\gamma_\nu-\gamma_\nu\gamma_\mu)q^\mu u_A\right)i\frac{g_{\nu\beta}-q_\nu q_\beta/m_V^2}{q^2-m_V^2}\frac{g}{4}(P_{B\beta}+P_{D\beta}), \quad (26)$$

$$\mathcal{M}_I^{(\rho,\omega,\phi,K^*)}(\Xi_c^*\bar{K}/\Omega_c^*\eta\to\Xi_c\bar{K})=\frac{\lambda_I g_V}{\sqrt{2}}(-\varepsilon^{\mu\nu\kappa\lambda}+\varepsilon^{\mu\nu\lambda\kappa})v_\mu\bar{u}_C q_\lambda u_{A\nu}(-i)\frac{g^{\kappa\beta}-q^\kappa q^\beta/m_V^2}{q^2-m_V^2}\frac{g}{4}(P_{B\beta}+P_{D\beta}), \quad (27)$$

$$\mathcal{M}_I^{(\rho,\omega,\phi,K^*)}(\Xi_c^*\bar{K}/\Omega_c^*\eta\to\Xi_c'\bar{K})=\left(\frac{\beta_S g_V}{\sqrt{6}}\bar{u}_C\gamma^5(\gamma_\mu+v_\mu)v_\alpha u_A^\mu-\frac{\lambda_S g_V}{\sqrt{6}}\bar{u}_C\gamma^5 q^\mu[(\gamma_\mu+v_\mu)u_{A\alpha}-(\gamma_\alpha+v_\alpha)u_{A\mu}]\right)\times\frac{-g^{\alpha\beta}+q^\alpha q^\beta/m_V^2}{q^2-m_V^2}\frac{g}{4}(P_{B\beta}+P_{D\beta}), \quad (28)$$

TABLE V. Allowed two-body decay widths for the predicted Ω_c state.

Λ (GeV)	E (MeV)	$\Gamma_{\Omega_c(3140)\to\Xi_c\bar{K}}$ (MeV)	$\Gamma_{\Omega_c(3140)\to\Xi_c'\bar{K}}$ (MeV)	Γ_{total} (MeV)
1.270	−0.58	~0	0.060	0.060
1.320	−6.00	0.002	1.909	1.911
1.370	−20.55	0.005	16.360	16.365

$$\mathcal{M}_I^{(\rho,\omega,\phi)}(\Xi_c\bar{K}^*\to\Xi_c\bar{K}) = \frac{\beta_B g_V}{\sqrt{2}}\bar{u}_C u_A v_\kappa(-i)\frac{g^{\kappa\beta}-q^\kappa q^\beta/m_V^2}{q^2-m_V^2}\frac{g_{VVP}}{4}\varepsilon_{\mu\nu\alpha\beta}P_B^\mu\epsilon_B^\nu q^\alpha, \tag{29}$$

$$\mathcal{M}_I^{(\rho,\omega,\phi)}(\Xi_c\bar{K}^*\to\Xi_c'\bar{K}) = \frac{\lambda_I g_V}{\sqrt{6}}(\varepsilon^{\mu\nu\lambda\kappa}-\varepsilon^{\mu\nu\kappa\lambda})v_\mu\bar{u}_C\gamma^5\gamma_\nu q_\lambda u_A\frac{g_{\kappa\beta}-q_\kappa q_\beta/m_V^2}{q^2-m_V^2}\frac{g_{VVP}}{4}\varepsilon_{\sigma\gamma\alpha\beta}P_B^\sigma\epsilon_B^\gamma q^\alpha, \tag{30}$$

$$\mathcal{M}_I^{\pi}(\Xi_c\bar{K}^*\to\Xi_c'\bar{K}) = \frac{1}{\sqrt{3}}\frac{g_4}{f_\pi}\bar{u}_C\gamma^5(\gamma^\mu+v^\mu)(q_\mu)u_A\frac{1}{q^2-m_\pi^2}\frac{g}{4}\epsilon_B^\nu(q_\nu+P_{D\nu}), \tag{31}$$

$$\mathcal{M}_I^{(\rho,\omega,\phi,K^*)}(\Xi_c'\bar{K}^*/\Omega_c\omega\to\Xi_c\bar{K}) = \frac{\lambda_I g_V}{\sqrt{6}}(\varepsilon^{\mu\nu\lambda\kappa}-\varepsilon^{\mu\nu\kappa\lambda})v_\mu\bar{u}_C\gamma^5\gamma_\nu q_\lambda u_A\frac{g_{\kappa\beta}-q_\kappa q_\beta/m_V^2}{q^2-m_V^2}\frac{g_{VVP}}{4}\varepsilon_{\sigma\gamma\alpha\beta}P_B^\sigma\epsilon_B^\gamma q^\alpha, \tag{32}$$

$$\mathcal{M}_I^{\pi,K}(\Xi_c'\bar{K}^*/\Omega_c\omega\to\Xi_c\bar{K}) = \frac{1}{\sqrt{3}}\frac{g_4}{f_\pi}\bar{u}_C\gamma^5(\gamma^\mu+v^\mu)(q_\mu)u_A\frac{1}{q^2-m_\pi^2}\frac{g}{4}\epsilon_B^\nu(q_\nu+P_{D\nu}), \tag{33}$$

$$\mathcal{M}_I^{(\rho,\omega,\phi,K^*)}(\Xi_c'\bar{K}^*/\Omega_c\omega\to\Xi_c'\bar{K}) = \left(\frac{\beta_S g_V}{\sqrt{2}}\bar{u}_C u_A v_\nu-\frac{\lambda_S g_V}{3\sqrt{2}}\bar{u}_C(\gamma_\mu\gamma_\nu-\gamma_\nu\gamma_\mu)q^\mu u_A\right)i\frac{g_{\nu\beta}-q_\nu q_\beta/m_V^2}{q^2-m_V^2}\frac{g_{VVP}}{4}\varepsilon_{\kappa\sigma\alpha\beta}P_B^\kappa\epsilon_B^\sigma q^\alpha, \tag{34}$$

$$\mathcal{M}_I^{\pi,K}(\Xi_c'\bar{K}^*/\Omega_c\omega\to\Xi_c'\bar{K}) = \frac{g_1}{2f_\pi}\varepsilon^{\mu\nu\lambda\kappa}v_\kappa\bar{u}_C\gamma_\mu\gamma_\lambda q_\nu u_1\frac{i}{q^2-m_\pi^2}\frac{g}{4}\epsilon_B^\alpha(q_\alpha+P_{D\alpha}). \tag{35}$$

In Table IV, using the wave function of the $\Xi_c^*\bar{K}/\Omega_c\eta/\Omega_c^*\eta/\Xi_c\bar{K}^*/\Xi_c'\bar{K}^*/\Omega_c\omega$ state with $I(J^P)=0(3/2^-)$, the decay widths for all of the allowed decay channels are collected into three groups, which are based on the choices of the cutoff Λ.

In Table V, the total decay width for the $\Xi_c^*\bar{K}/\Omega_c\eta/\Omega_c^*\eta/\Xi_c\bar{K}^*/\Xi_c'\bar{K}^*/\Omega_c\omega$ state with $I(J^P)=0(3/2^-)$ is around several MeV, and $\Xi_c'\bar{K}$ is the dominant decay channel. As the cutoff increases, the total decay width becomes larger. For the $\Xi_c\bar{K}$ channel, the decay width is less than 1 MeV. A measurement in the $\Xi_c'\bar{K}$ channel is helpful to further understand the structure of Ω_c states.

IV. OTHER PARTNERS

After we discuss the isoscalar $\Xi_c^*\bar{K}/\Omega_c\eta/\Omega_c^*\eta/\Xi_c\bar{K}^*/\Xi_c'\bar{K}^*/\Omega_c\omega$ systems, in the following we study their isovector partners by using the same model. The $\Xi_c^*\bar{K}$, $\Xi_c\bar{K}^*$, $\Xi_c'\bar{K}^*$, and $\Omega_c\rho$ channels are considered. The corresponding numerical results are presented in Table VI.

Finally, we find that the $\Xi_c^*\bar{K}/\Xi_c\bar{K}^*/\Xi_c'\bar{K}^*/\Omega_c\rho$ state with $I(J^P)=1(3/2^-)$ may be the other loosely bound molecular state, where the $\Xi_c^*\bar{K}$ channel is also dominant. For $I(J^P)=1(1/2^\pm)$, $1(3/2^+)$, and $1(5/2^\pm)$, because the value of the cutoff Λ is away from 1 GeV and/or their rms radii are very small, they are no possible loose molecular candidates.

As a byproduct, we further extend our study on the Ξ_c^*K system. According to the G-parity rule [55], the properties of the ω and ϕ exchanges are exactly opposite to those in the $\Xi_c^*\bar{K}$ system. After solving the Schrödinger equation, our results indicate the following.

(1) For the isoscalar Ξ_c^*K system, bound solutions can be obtained when the cutoff is taken larger than 1.7 GeV. Thus, the interaction from the single channel is not strong enough to generate a loosely bound state.

(2) For the isovector Ξ_c^*K system, there are no binding solutions when we tune the cutoff Λ from 1 to 5 GeV.

Finally, when the $\Xi_c^*K/\Sigma_c\rho/\Sigma_c\omega/\Sigma_c^*\rho/\Sigma_c^*\omega/\Xi_cK^*/\Xi_c'K^*$ coupled-channel system is further considered, we can predict two possible loosely bound molecular states: the isoscalar $\Xi_c^*K/\Sigma_c\rho/\Sigma_c^*\rho/\Xi_cK^*/\Xi_c'K^*$ state with $J^P=3/2^-$ and the isovector $\Xi_c^*K/\Sigma_c\rho/\Sigma_c\omega/\Sigma_c^*\rho/\Sigma_c^*\omega/\Xi_cK^*/\Xi_c'K^*$ state with $J^P=3/2^-$. For the isoscalar state, the Ξ_c^*K channel is dominant with a greater than 80% probability. For the isovector state, the remaining channels

TABLE VI. Bound-state properties (binding energy E and root-mean-square radius r_{rms}) for all of the investigated systems after the coupled-channel effects are considered. The probabilities for the different channels are also given. E, r_{rms}, and Λ are in units of MeV, fm, and GeV, respectively. To emphasize the dominant channel, we label the probability for the corresponding channel in bold.

$I(J^P)$	Λ	E	r_{rms}	$\Xi_c^*\bar{K}(\%)$	$\Xi_c\bar{K}^*(\%)$	$\Xi_c'\bar{K}^*(\%)$	$\Omega_c\rho(\%)$
$1(1/2^-)$	1.656	−0.96	0.36	0.61	**46.95**	**50.48**	1.85
	1.660	−5.06	0.35	0.60	**46.82**	**50.72**	1.98
	1.664	−9.21	0.35	0.60	**46.45**	**50.94**	2.00
$1(1/2^+)$	1.820	−0.46	0.75	8.31	**55.20**	20.41	16.07
	1.824	−3.40	0.63	7.70	**55.39**	20.46	16.19
	1.828	−6.36	0.60	7.36	**55.65**	20.51	16.46
$1(3/2^-)$	1.460	−0.67	4.85	**95.89**	3.60	0.24	0.27
	1.510	−4.32	2.37	**90.00**	8.71	0.53	0.76
	1.560	−11.35	1.47	**81.86**	13.93	0.79	1.42
$1(3/2^+)$	2.230	−1.90	0.48	4.58	23.55	**48.32**	23.53
	2.232	−4.26	0.45	4.43	23.51	**48.44**	23.61
	2.234	−6.63	0.44	4.32	23.45	**48.53**	23.68
$1(5/2^-)$	2.812	−0.90	0.40	0.61	20.58	**56.55**	22.26
	2.816	−5.34	0.40	0.61	20.48	**56.58**	22.31
	2.816	−5.34	0.40	0.61	20.40	**55.60**	22.38
$1(5/2^+)$	3.590	−1.27	0.43	0.92	**37.30**	**26.38**	**35.39**
	3.600	−4.76	0.42	0.88	**37.25**	**26.39**	**35.48**
	3.610	−8.28	0.42	0.85	**37.19**	**26.39**	**35.56**

$\Sigma_c\rho/\Sigma_c\omega/\Sigma_c^*\rho/\Sigma_c^*\omega/\Xi_cK^*/\Xi_c'K^*$ play much more important roles, due to their larger probabilities.

V. SUMMARY

Since the observation of the hidden-charm pentaquarks $P_c(4380)$ and $P_c(4450)$, the search for heavy pentaquarks has become a very hot topic in hadron physics. In this work, by adopting the OBE model and coupled-channel effect, we carried out a systematic investigation of possible Ω_c-like molecular states from the $\Xi_c^*\bar{K}/\Omega_c\eta/\Omega_c^*\eta/\Xi_c\bar{K}^*/\Xi_c'\bar{K}^*/\Omega_c\omega$ interaction.

In order to justify the existence of a molecular state, we borrowed knowledge gained from studies of the deuteron. We found a reasonable loose Ω_c-like molecular state: the $\Xi_c^*\bar{K}/\Omega_c\eta/\Omega_c^*\eta/\Xi_c\bar{K}^*/\Xi_c'\bar{K}^*/\Omega_c\omega$ state with $I(J^P)=0(3/2^-)$. Compared to the probabilities for all of the discussed channels, it is mainly made up of the S-wave $\Xi_c^*\bar{K}$ component. Then, we further studied the two-body strong decay behavior of the $\Xi_c^*\bar{K}/\Omega_c\eta/\Omega_c^*\eta/\Xi_c\bar{K}^*/\Xi_c'\bar{K}^*/\Omega_c\omega$ state with $I(J^P)=0(3/2^-)$. Our results indicate that its two-body strong decay width is around several MeV, and the $\Xi_c'\bar{K}$ decay channel is dominant. In comparison with the observation by the LHCb Collaboration [43], the mass of this $\Xi_c^*\bar{K}/\Omega_c\eta/\Omega_c^*\eta/\Xi_c\bar{K}^*/\Xi_c'\bar{K}^*/\Omega_c\omega$ state with $I(J^P)=0(3/2^-)$ is very close to their threshold, especially for $\Omega_c(3090)$ and $\Omega_c(3119)$. If the spin parities of the five Ω_c states are further determined in the future, the Ω_c with $I(J^P)=0(3/2^-)$ can be easily related to the $\Xi_c^*\bar{K}/\Omega_c\eta/\Omega_c^*\eta/\Xi_c\bar{K}^*/\Xi_c'\bar{K}^*/\Omega_c\omega$ state with $I(J^P)=0(3/2^-)$. Meanwhile, we may predict an isovector molecular partner: the $\Xi_c^*\bar{K}/\Xi_c\bar{K}^*/\Xi_c'\bar{K}^*/\Omega_c\rho$ state with $I(J^P)=1(3/2^-)$.

ACKNOWLEDGMENTS

This project is partly supported by the National Natural Science Foundation of China under Grants No. 11222547, No. 11175073, and No. 11647301, and the Fundamental Research Funds for the Central Universities. R. C. is supported by the China Scholarship Council. X. L. is also supported in part by the National Program for Support of Top-notch Young Professionals. A. H. is supported by the JSPS KAKENHI [the Grant-in-Aid for Scientific Research from the Japan Society for the Promotion of Science (JSPS)] with Grant No. JP26400273(C).

APPENDIX: RELEVANT SUBPOTENTIALS

The exact subpotentials in Eq. (21) are expressed as

$$\mathcal{V}_{I,J^P}^{\Xi_c^*\bar{K}\to\Xi_c^*\bar{K}}(r)=-\frac{1}{2}l_Sg_\sigma\mathcal{D}_1(J^P)Y(\Lambda,m_\sigma,r)-\frac{1}{16}\beta_Sg_Vg\mathcal{D}_1(J^P)[\mathcal{G}(I)Y(\Lambda,m_\rho,r)+Y(\Lambda,m_\omega,r)-2Y(\Lambda,m_\phi,r)], \quad (A1)$$

$$\mathcal{V}_{I,J^P}^{\Xi_c\bar{K}^*\to\Xi_c^*\bar{K}}(r)=\frac{1}{8}\frac{g_4 g}{f_\pi}\frac{1}{\sqrt{M_{\bar{K}}M_{\bar{K}^*}}}\left[\frac{1}{3}\mathcal{E}_1(J^P)\nabla^2+\frac{1}{3}\mathcal{F}_1(J^P)r\frac{\partial}{\partial r}\frac{1}{r}\frac{\partial}{\partial r}\right]\mathcal{G}(I)U(\Lambda_0,m_{\pi 0},r)$$
$$-\frac{1}{8}\frac{g_4 g}{f_\pi}\frac{1}{\sqrt{M_{\bar{K}}M_{\bar{K}^*}}}\left[\frac{1}{3}\mathcal{E}_1(J^P)\nabla^2+\frac{1}{3}\mathcal{F}_1(J^P)r\frac{\partial}{\partial r}\frac{1}{r}\frac{\partial}{\partial r}\right]Y(\Lambda_0,m_{\eta 0},r)$$
$$-\frac{\lambda_I g_V g_{VVP}}{2\sqrt{2}}\left[\frac{2}{3}\mathcal{E}_1(J^P)\nabla^2-\frac{1}{3}\mathcal{F}_1(J^P)r\frac{\partial}{\partial r}\frac{1}{r}\frac{\partial}{\partial r}\right][\mathcal{G}(I)Y(\Lambda_0,m_{\rho 0},r)+Y(\Lambda_0,m_{\omega 0},r)-2Y(\Lambda_0,m_{\phi 0},r)], \quad \text{(A2)}$$

$$\mathcal{V}_{I,J^P}^{\Xi_c'\bar{K}^*\to\Xi_c^*\bar{K}}(r)=-\frac{\sqrt{3}}{16\sqrt{2}}\frac{g_1 g}{f_\pi}\frac{1}{\sqrt{M_{\bar{K}}M_{\bar{K}^*}}}\left[\frac{1}{3}\mathcal{E}_1(J^P)\nabla^2+\frac{1}{3}\mathcal{F}_1(J^P)r\frac{\partial}{\partial r}\frac{1}{r}\frac{\partial}{\partial r}\right]\mathcal{G}(I)U(\Lambda_1,m_{\pi 1},r)$$
$$-\frac{\sqrt{3}}{48\sqrt{2}}\frac{g_1 g}{f_\pi}\frac{1}{\sqrt{M_{\bar{K}}M_{\bar{K}^*}}}\left[\frac{1}{3}\mathcal{E}_1(J^P)\nabla^2+\frac{1}{3}\mathcal{F}_1(J^P)r\frac{\partial}{\partial r}\frac{1}{r}\frac{\partial}{\partial r}\right]Y(\Lambda_1,m_{\eta 1},r)$$
$$-\frac{\lambda_S g_V g_{VVP}}{8\sqrt{3}}\left[\frac{2}{3}\mathcal{E}_1(J^P)\nabla^2-\frac{1}{3}\mathcal{F}_1(J^P)r\frac{\partial}{\partial r}\frac{1}{r}\frac{\partial}{\partial r}\right][\mathcal{G}(I)Y(\Lambda_1,m_{\rho 1},r)+Y(\Lambda_1,m_{\omega 1},r)-2Y(\Lambda_1,m_{\phi 1},r)], \quad \text{(A3)}$$

$$\mathcal{V}_{I,J^P}^{\Xi_c\bar{K}^*\to\Xi_c\bar{K}^*}(r)=2l_B g_\sigma\mathcal{D}_2(J^P)Y(\Lambda,m_\sigma,r)+\frac{1}{8}\beta_B g_V g\mathcal{D}_2(J^P)[\mathcal{G}(I)Y(\Lambda,m_\rho,r)+Y(\Lambda,m_\omega,r)-2Y(\Lambda,m_\phi,r)], \quad \text{(A4)}$$

$$\mathcal{V}_{I,J^P}^{\Xi_c\bar{K}^*\to\Xi_c'\bar{K}^*}(r)=\frac{1}{4\sqrt{3}}\frac{g_4 g_{VVP}}{f_\pi}\left[\frac{1}{3}\mathcal{E}_2(J^P)\nabla^2+\frac{1}{3}\mathcal{F}_2(J^P)r\frac{\partial}{\partial r}\frac{1}{r}\frac{\partial}{\partial r}\right]\mathcal{G}(I)Y(\Lambda_2,m_{\pi 2},r)$$
$$-\frac{1}{4\sqrt{3}}\frac{g_4 g_{VVP}}{f_\pi}\left[\frac{1}{3}\mathcal{E}_2(J^P)\nabla^2+\frac{1}{3}\mathcal{F}_2(J^P)r\frac{\partial}{\partial r}\frac{1}{r}\frac{\partial}{\partial r}\right]Y(\Lambda_2,m_{\eta 2},r)$$
$$+\frac{1}{4\sqrt{6}}\lambda_I g_V g\frac{1}{M_{\bar{K}^*}}\mathcal{H}_1(J^P)\frac{1}{r}\frac{\partial}{\partial r}[\mathcal{G}(I)Y(\Lambda_2,m_{\rho 2},r)+Y(\Lambda_2,m_{\omega 2},r)-2Y(\Lambda_2,m_{\phi 2},r)]$$
$$+\frac{\lambda_I g_V g}{4\sqrt{6}M_{\bar{K}^*}}\left[\frac{2}{3}\mathcal{E}_2(J^P)\nabla^2-\frac{1}{3}\mathcal{F}_2(J^P)r\frac{\partial}{\partial r}\frac{1}{r}\frac{\partial}{\partial r}\right][\mathcal{G}(I)Y(\Lambda_2,m_{\rho 2},r)+Y(\Lambda_2,m_{\omega 2},r)-2Y(\Lambda_2,m_{\phi 2},r)], \quad \text{(A5)}$$

$$\mathcal{V}_{I,J^P}^{\Xi_c'\bar{K}^*\to\Xi_c'\bar{K}^*}(r)=-\frac{1}{2}g_\sigma l_S\mathcal{D}_2(J^P)Y(\Lambda,m_\sigma,r)+\frac{\sqrt{3}}{8\sqrt{2}}\frac{g_1 g_{VVP}}{f_\pi}\left[\frac{1}{3}\mathcal{E}_2(J^P)\nabla^2+\frac{1}{3}\mathcal{F}_2(J^P)r\frac{\partial}{\partial r}\frac{1}{r}\frac{\partial}{\partial r}\right]\mathcal{G}(I)Y(\Lambda,m_\pi,r)$$
$$+\frac{\sqrt{3}}{24\sqrt{2}}\frac{g_1 g_{VVP}}{f_\pi}\left[\frac{1}{3}\mathcal{E}_2(J^P)\nabla^2+\frac{1}{3}\mathcal{F}_2(J^P)r\frac{\partial}{\partial r}\frac{1}{r}\frac{\partial}{\partial r}\right]Y(\Lambda,m_\eta,r)$$
$$-\frac{1}{16}\beta_S g_V g\mathcal{D}_2(J^P)[\mathcal{G}(I)Y(\Lambda,m_\rho,r)+Y(\Lambda,m_\omega,r)-2Y(\Lambda,m_\phi,r)]$$
$$-\frac{1}{48}\frac{\lambda_S g_V g}{M_{\Xi_c'}}\mathcal{D}_2(J^P)[\mathcal{G}(I)\nabla^2Y(\Lambda,m_\rho,r)+\nabla^2Y(\Lambda,m_\omega,r)-2\nabla^2Y(\Lambda,m_\phi,r)]$$
$$+\frac{1}{24}\frac{\lambda_S g_V g}{M_{\bar{K}^*}}\mathcal{H}_1(J^P)\frac{1}{r}\frac{\partial}{\partial r}[\mathcal{G}(I)Y(\Lambda,m_\rho,r)+Y(\Lambda,m_\omega,r)-2Y(\Lambda,m_\phi,r)]$$
$$-\frac{1}{24}\frac{\lambda_S g_V g}{M_{\bar{K}^*}}\left[\frac{2}{3}\mathcal{E}_2(J^P)\nabla^2-\frac{1}{3}\mathcal{F}_2(J^P)r\frac{\partial}{\partial r}\frac{1}{r}\frac{\partial}{\partial r}\right][\mathcal{G}(I)Y(\Lambda,m_\rho,r)+Y(\Lambda,m_\omega,r)-2Y(\Lambda,m_\phi,r)], \quad \text{(A6)}$$

$$\mathcal{V}_{I,J^P}^{\Xi_c^*\bar{K}\to\Omega_c\eta}(r)=\frac{1}{8\sqrt{2}}\beta_S g_V g\mathcal{D}_3(J^P)Y(\Lambda_3,m_{K^*3},r)+\frac{1}{8\sqrt{2}}\frac{\lambda_S g_V g}{\sqrt{m_\eta m_K}}\mathcal{H}_2(J^P)\frac{1}{r}\frac{\partial}{\partial r}Y(\Lambda_3,m_{K^*3},r), \quad \text{(A7)}$$

$$\mathcal{V}_{I,J^P}^{\Xi_c^*\bar{K}\to\Omega_c^*\eta}(r)=-\frac{1}{4\sqrt{6}}\beta_S g_V g\mathcal{D}_1(J^P)Y(\Lambda_4,m_{K^*4},r), \quad \text{(A8)}$$

$$\mathcal{V}_{I,J^P}^{\Omega_c\omega\to\Xi_c^*\bar{K}}(r) = \frac{\sqrt{3}}{8}\frac{g_1 g}{f_\pi}\frac{1}{\sqrt{m_\omega m_K}}\left[\frac{1}{3}\mathcal{E}_1(J^P)\nabla^2 + \frac{1}{3}\mathcal{F}_1(J^P)r\frac{\partial}{\partial r}\frac{1}{r}\frac{\partial}{\partial r}\right]Y(\Lambda_5, m_{K5}, r) + \frac{\sqrt{6}}{12}\lambda_S g_V g_{VVP}\left[\frac{2}{3}\mathcal{E}_1(J^P)\nabla^2 - \frac{1}{3}\mathcal{F}_1(J^P)r\frac{\partial}{\partial r}\frac{1}{r}\frac{\partial}{\partial r}\right]Y(\Lambda_5, m_{K^*5}, r), \tag{A9}$$

$$\mathcal{V}_{I,J^P}^{\Omega_c\eta\to\Omega_c\eta}(r) = \frac{1}{6\sqrt{2}}\beta_S g_V g Y(\Lambda, m_\phi, r) + \frac{1}{18\sqrt{2}}\frac{\lambda_S g_V g}{M_{\Omega_c}}\nabla^2 Y(\Lambda, m_\phi, r), \tag{A10}$$

$$\mathcal{V}_{I,J^P}^{\Omega_c^*\eta\to\Omega_c\eta}(r) = -\frac{1}{6\sqrt{6}}\beta_S g_V g \mathcal{D}_2(J^P) Y(\Lambda_6, m_{\phi 6}, r) - \frac{1}{6\sqrt{6}}\frac{\lambda_S g_V g}{m_\eta}\mathcal{H}_2(J^P)\frac{1}{r}\frac{\partial}{\partial r}Y(\Lambda_6, m_{\phi 6}, r), \tag{A11}$$

$$\mathcal{V}_{I,J^P}^{\Omega_c\omega\to\Omega_c\eta}(r) = -\frac{1}{12\sqrt{3}}\frac{g_1 g}{f_\pi}\left[\frac{1}{3}\mathcal{E}_3(J^P)\nabla^2 + \frac{1}{3}\mathcal{F}_3(J^P)r\frac{\partial}{\partial r}\frac{1}{r}\frac{\partial}{\partial r}\right]Y(\Lambda_7, m_{\eta 7}, r), \tag{A12}$$

$$\mathcal{V}_{I,J^P}^{\Xi_c\bar{K}^*\to\Omega_c\eta}(r) = \frac{1}{6\sqrt{2}}\frac{g_4 g}{f_\pi}\frac{1}{\sqrt{m_\eta m_{K^*}}}\left[\frac{1}{3}\mathcal{E}_3(J^P)\nabla^2 + \frac{1}{3}\mathcal{F}_3(J^P)r\frac{\partial}{\partial r}\frac{1}{r}\frac{\partial}{\partial r}\right]Y(\Lambda_8, m_{K8}, r) + \frac{1}{12}\lambda_I g_V g_{VVP}\sqrt{\frac{m_{K^*}}{m_\eta}}\left[\frac{2}{3}\mathcal{E}_3(J^P)\nabla^2 - \frac{1}{3}\mathcal{F}_3(J^P)r\frac{\partial}{\partial r}\frac{1}{r}\frac{\partial}{\partial r}\right]Y(\Lambda_8, m_{K^*8}, r), \tag{A13}$$

$$\mathcal{V}_{I,J^P}^{\Xi_c'\bar{K}^*\to\Omega_c\eta}(r) = -\frac{1}{4\sqrt{3}}\frac{g_1 g}{f_\pi}\frac{1}{\sqrt{m_\eta m_{K^*}}}\left[\frac{1}{3}\mathcal{E}_3(J^P)\nabla^2 + \frac{1}{3}\mathcal{F}_3(J^P)r\frac{\partial}{\partial r}\frac{1}{r}\frac{\partial}{\partial r}\right]Y(\Lambda_9, m_{K9}, r) + \frac{1}{4\sqrt{6}}\frac{\beta_S g_V g_{VVP}}{\sqrt{m_\eta m_{K^*}}}\mathcal{H}_3(J^P)\frac{1}{r}\frac{\partial}{\partial r}Y(\Lambda_9, m_{K^*9}, r) + \frac{1}{12\sqrt{6}}\lambda_S g_V g_{VVP}\sqrt{\frac{m_{K^*}}{m_\eta}}\left[\frac{2}{3}\mathcal{E}_3(J^P)\nabla^2 - \frac{1}{3}\mathcal{F}_3(J^P)r\frac{\partial}{\partial r}\frac{1}{r}\frac{\partial}{\partial r}\right]Y(\Lambda_9, m_{K^*9}, r), \tag{A14}$$

$$\mathcal{V}_{I,J^P}^{\Omega_c^*\eta\to\Omega_c^*\eta}(r) = \frac{1}{6\sqrt{2}}\beta_S g_V g \mathcal{D}_1(J^P) Y(\Lambda, m_\phi, r), \tag{A15}$$

$$\mathcal{V}_{I,J^P}^{\Xi_c\bar{K}^*\to\Omega_c^*\eta}(r) = \sqrt{\frac{2}{3}}\frac{g_4 g}{f_\pi}\frac{1}{\sqrt{m_\eta m_{K^*}}}\left[\frac{1}{3}\mathcal{E}_1(J^P)\nabla^2 + \frac{1}{3}\mathcal{F}_1(J^P)r\frac{\partial}{\partial r}\frac{1}{r}\frac{\partial}{\partial r}\right]Y(\Lambda_{10}, m_{K10}, r) - \frac{1}{\sqrt{3}}\lambda_I g_V g_{VVP}\left[\frac{2}{3}\mathcal{E}_1(J^P)\nabla^2 - \frac{1}{3}\mathcal{F}_1(J^P)r\frac{\partial}{\partial r}\frac{1}{r}\frac{\partial}{\partial r}\right]Y(\Lambda_{10}, m_{K^*10}, r), \tag{A16}$$

$$\mathcal{V}_{I,J^P}^{\Xi_c'\bar{K}^*\to\Omega_c^*\eta}(r) = -\frac{1}{8}\frac{g_1 g}{f_\pi}\frac{1}{\sqrt{m_\eta m_{K^*}}}\left[\frac{1}{3}\mathcal{E}_1(J^P)\nabla^2 + \frac{1}{3}\mathcal{F}_1(J^P)r\frac{\partial}{\partial r}\frac{1}{r}\frac{\partial}{\partial r}\right]Y(\Lambda_{11}, m_{K11}, r) - \frac{1}{12}\lambda_S g_V g_{VVP}\left[\frac{2}{3}\mathcal{E}_1(J^P)\nabla^2 - \frac{1}{3}\mathcal{F}_1(J^P)r\frac{\partial}{\partial r}\frac{1}{r}\frac{\partial}{\partial r}\right]Y(\Lambda_{11}, m_{K^*11}, r), \tag{A17}$$

$$\mathcal{V}_{I,J^P}^{\Omega_c\omega\to\Omega_c\omega}(r) = \frac{1}{4\sqrt{3}}\frac{g_1 g_{VVP}}{f_\pi}\left[\frac{1}{3}\mathcal{E}_2(J^P)\nabla^2 + \frac{1}{3}\mathcal{F}_2(J^P)r\frac{\partial}{\partial r}\frac{1}{r}\frac{\partial}{\partial r}\right]Y(\Lambda, m_\eta, r), \tag{A18}$$

$$\mathcal{V}_{I,J^P}^{\Xi_c\bar{K}^*\to\Omega_c\omega}(r) = -\frac{1}{\sqrt{6}}\frac{g_4 g_{VVP}}{f_\pi}\left[\frac{1}{3}\mathcal{E}_2(J^P)\nabla^2 + \frac{1}{3}\mathcal{F}_2(J^P) r\frac{\partial}{\partial r}\frac{1}{r}\frac{\partial}{\partial r}\right]Y(\Lambda_{12}, m_{K12}, r)$$
$$+\frac{1}{2\sqrt{3}}\frac{\lambda_I g_V g}{\sqrt{m_{K^*}m_\omega}}\mathcal{H}_1(J^P)\frac{1}{r}\frac{\partial}{\partial r}Y(\Lambda_{12}, m_{K^*12}, r)$$
$$+\frac{1}{2\sqrt{3}}\frac{\lambda_I g_V g}{\sqrt{m_{K^*}m_\omega}}\left[\frac{2}{3}\mathcal{E}_2(J^P)\nabla^2 - \frac{1}{3}\mathcal{F}_2(J^P) r\frac{\partial}{\partial r}\frac{1}{r}\frac{\partial}{\partial r}\right]Y(\Lambda_{12}, m_{K^*12}, r), \quad \text{(A19)}$$

$$\mathcal{V}_{I,J^P}^{\Xi_c'\bar{K}^*\to\Omega_c\omega}(r) = -\frac{\sqrt{3}}{4}\frac{g_1 g_{VVP}}{f_\pi}\left[\frac{1}{3}\mathcal{E}_2(J^P)\nabla^2 + \frac{1}{3}\mathcal{F}_2(J^P) r\frac{\partial}{\partial r}\frac{1}{r}\frac{\partial}{\partial r}\right]Y(\Lambda_{13}, m_{K13}, r) + \frac{1}{4\sqrt{2}}\beta_S g_V g\mathcal{D}_2(J^P)Y(\Lambda_{12}, m_{K^*12}, r)$$
$$+\frac{1}{12\sqrt{2}}\lambda_S g_V g\mathcal{D}_2(J^P)\nabla^2 Y(\Lambda_{13}, m_{K^*13}, r) - \frac{1}{6\sqrt{2}}\frac{\lambda_S g_V g}{\sqrt{m_\omega m_{K^*}}}\mathcal{H}_1(J^P)\frac{1}{r}\frac{\partial}{\partial r}Y(\Lambda_{12}, m_{K^*13}, r)$$
$$+\frac{1}{6\sqrt{2}}\frac{\lambda_S g_V g}{\sqrt{m_\omega m_{K^*}}}\left[\frac{2}{3}\mathcal{E}_2(J^P)\nabla^2 - \frac{1}{3}\mathcal{F}_2(J^P) r\frac{\partial}{\partial r}\frac{1}{r}\frac{\partial}{\partial r}\right]Y(\Lambda_{13}, m_{K^*13}, r). \quad \text{(A20)}$$

In Eq. (A1), the function $U(\Lambda_i, m_{\pi i}, r)$ is defined as

$$U(\Lambda_i, m_{\pi i}, r) = \frac{1}{4\pi r}(\cos(m_{\pi i} r) - e^{-\Lambda_i r}) - \frac{\Lambda_i^2 + m_{\pi i}^2}{8\pi\Lambda_i}e^{-\Lambda_i r}, \qquad i = 0, 1, 2.$$

The variables in Eqs. (A1)–(A20) are

$$q_0 = \frac{M_{\Xi_c^*}^2 + M_{\bar{K}^*}^2 - M_{\Xi_c}^2 - M_K^2}{2(M_{\Xi_c^*} + M_{\bar{K}})}, \qquad q_1 = \frac{M_{\Xi_c^*}^2 + M_{\bar{K}^*}^2 - M_{\Xi_c'}^2 - M_K^2}{2(M_{\Xi_c^*} + M_{\bar{K}})}, \qquad q_2 = \frac{M_{\Xi_c'}^2 - M_{\Xi_c}^2}{2(M_{\Xi_c} + M_{\bar{K}^*}^2)},$$
$$q_3 = \frac{M_{\Xi_c^*}^2 - M_K^2 + m_\eta^2 - M_{\Omega_c}^2}{2(M_{\Xi_c^*} + M_{\bar{K}})}, \qquad q_4 = \frac{M_{\Xi_c^*}^2 - M_K^2 + m_\eta^2 - M_{\Omega_c^*}^2}{2(M_{\Xi_c^*} + M_{\bar{K}})}, \qquad q_5 = \frac{M_{\Xi_c^*}^2 - M_K^2 + m_\omega^2 - M_{\Omega_c}^2}{2(M_{\Xi_c^*} + M_{\bar{K}})},$$
$$q_6 = \frac{-M_{\Omega_c}^2 + M_{\Omega_c^*}^2}{2(M_{\Omega_c} + M_\eta)}, \qquad q_7 = \frac{-M_\eta^2 + M_\omega^2}{2(M_{\Omega_c} + M_\eta)}, \qquad q_8 = \frac{M_{\Omega_c}^2 - M_\eta^2 + M_{K^*}^2 - M_{\Xi_c}^2}{2(M_{\Omega_c} + M_\eta)}, \qquad q_9 = \frac{M_{\Omega_c}^2 - M_\eta^2 + M_{K^*}^2 - M_{\Xi_c'}^2}{2(M_{\Omega_c} + M_\eta)},$$
$$q_{10} = \frac{M_{\Omega_c^*}^2 - M_\eta^2 + M_{K^*}^2 - M_{\Xi_c}^2}{2(M_{\Omega_c^*} + M_\eta)}, \qquad q_{11} = \frac{M_{\Omega_c^*}^2 - M_\eta^2 + M_{K^*}^2 - M_{\Xi_c'}^2}{2(M_{\Omega_c^*} + M_\eta)}, \qquad q_{12} = \frac{M_{\Omega_c}^2 - M_\omega^2 + M_{K^*}^2 - M_{\Xi_c}^2}{2(M_{\Omega_c} + M_\omega)},$$
$$q_{13} = \frac{M_{\Omega_c}^2 - M_\omega^2 + M_{K^*}^2 - M_{\Xi_c'}^2}{2(M_{\Omega_c} + M_\omega)}, \qquad \Lambda_i^2 = \Lambda^2 - q_i^2, \qquad mE_i^2 = |mE^2 - q_i^2|. \quad \text{(A21)}$$

In addition, $\mathcal{D}_i(J^P)$, $\mathcal{E}_i(J^P)$, $\mathcal{F}_i(J^P)$, and $\mathcal{H}_i(J^P)$ in Eqs. (A1)–(A20) are the spin-spin, tensor, and spin-orbit operators, respectively. For example,

$$\mathcal{D}_1 = \sum_{a,b}^{m,n} C_{1/2,a;1,b}^{3/2,a+b} C_{1/2,m;1,n}^{3/2,m+n}\chi_3^{a\dagger}\chi_1^m\boldsymbol{\epsilon}_1^n\cdot\boldsymbol{\epsilon}_3^{b\dagger}, \qquad \mathcal{D}_2 = \chi_3^\dagger\chi_1\boldsymbol{\epsilon}_2\cdot\boldsymbol{\epsilon}_4^\dagger,$$
$$\mathcal{D}_3 = \sum_{a,b} C_{1/2,a;1,b}^{3/2,a+b}\chi_3^\dagger(\boldsymbol{\sigma}\cdot\boldsymbol{\epsilon}_{1b})\chi_{1a}, \qquad \mathcal{E}_1 = \sum_{m,n} C_{1/2,m;1,n}^{3/2,m+n}\chi_3^{m\dagger}\boldsymbol{\epsilon}_2\cdot(i\boldsymbol{\epsilon}_3^{n\dagger}\times\boldsymbol{\sigma})\chi_1,$$
$$\mathcal{E}_2 = \chi_3^\dagger\boldsymbol{\sigma}\cdot(i\boldsymbol{\epsilon}_2\times\boldsymbol{\epsilon}_4^\dagger)\chi_1, \qquad \mathcal{E}_3 = \chi_3^\dagger(\boldsymbol{\sigma}\cdot\boldsymbol{\epsilon}_2)\chi_1,$$
$$\mathcal{F}_1 = \sum_{m,n} C_{1/2,m;1,n}^{3/2,m+n}\chi_3^{m\dagger}S(\hat{r}, \boldsymbol{\epsilon}_2, i\boldsymbol{\epsilon}_3^{n\dagger}\times\boldsymbol{\sigma})\chi_1, \qquad \mathcal{F}_2 = \chi_3^\dagger S(\hat{r}, \boldsymbol{\sigma}, i\boldsymbol{\epsilon}_2\times\boldsymbol{\epsilon}_4^\dagger)\chi_1,$$
$$\mathcal{F}_3 = \chi_3^\dagger S(\hat{r}, \boldsymbol{\sigma}, \boldsymbol{\epsilon}_2)\chi_1, \qquad \mathcal{H}_1 = \chi_3^\dagger(\boldsymbol{\epsilon}_2\cdot\boldsymbol{\epsilon}_4^\dagger)(\boldsymbol{\sigma}\cdot\boldsymbol{L})\chi_1,$$
$$\mathcal{H}_2 = \sum_{a,b} C_{1/2,a;1,b}^{3/2,a+b}\chi_3^\dagger(-i\boldsymbol{\sigma}\times\boldsymbol{\epsilon}_1^b)\cdot\boldsymbol{L}\chi_{1a}, \qquad \mathcal{H}_3 = \chi_3^\dagger(\boldsymbol{L}\cdot\boldsymbol{\epsilon}_2)\chi_1,$$
$$S(\hat{r}, \boldsymbol{a}, \boldsymbol{b}) = 3(\hat{r}\cdot\boldsymbol{a})(\hat{r}\cdot\boldsymbol{b}) - \boldsymbol{a}\cdot\boldsymbol{b}. \quad \text{(A22)}$$

The subscripts (1, 2, 3, 4) in the polarization vector $\boldsymbol{\epsilon}$ and spin wave function χ correspond to the hadrons in the process $B(1)M(2) \to B(3)M(4)$, where B and M stand for the baryon and meson, respectively. When performing the numerical

TABLE VII. Nonzero matrix elements $\langle f|\mathcal{A}|i\rangle$ in various channels for the operators $\mathcal{A}$ in Eq. (A22).

$\mathcal{A}$	$1/2^-$	$1/2^+$	$3/2^-$	$3/2^+$	$5/2^-$	$5/2^+$
$\mathcal{D}_1$	(1)	(1)	$\begin{pmatrix}1&0\\0&1\end{pmatrix}$	(1)	(1)	(1)
$\mathcal{D}_2$	$\begin{pmatrix}1&0\\0&1\end{pmatrix}$	$\begin{pmatrix}1&0\\0&1\end{pmatrix}$	$\begin{pmatrix}1&0&0\\0&1&0\\0&0&1\end{pmatrix}$	$\begin{pmatrix}1&0\\0&1\end{pmatrix}$	$\begin{pmatrix}1&0\\0&1\end{pmatrix}$	(1)
$\mathcal{D}_3$	(0)	(0)	$\begin{pmatrix}0&\frac{2}{5\sqrt{3}}\end{pmatrix}$	$\begin{pmatrix}-\frac{2}{\sqrt{15}}\end{pmatrix}$	$\begin{pmatrix}-2\sqrt{\frac{2}{21}}\end{pmatrix}$	(0)
$\mathcal{E}_1$	$\begin{pmatrix}0&1\end{pmatrix}$	$\begin{pmatrix}0&1\end{pmatrix}$	$\begin{pmatrix}1&0&0\\0&0&1\end{pmatrix}$	$\begin{pmatrix}0&1\end{pmatrix}$	$\begin{pmatrix}0&1\end{pmatrix}$	(1)
$\mathcal{E}_2$	$\begin{pmatrix}-2&0\\0&1\end{pmatrix}$	$\begin{pmatrix}-2&0\\0&1\end{pmatrix}$	$\begin{pmatrix}1&0&0\\0&-2&0\\0&0&1\end{pmatrix}$	$\begin{pmatrix}-2&0\\0&1\end{pmatrix}$	$\begin{pmatrix}-2&0\\0&1\end{pmatrix}$	(1)
$\mathcal{E}_3$	$\begin{pmatrix}\sqrt{3}&0\end{pmatrix}$	$\begin{pmatrix}\sqrt{3}&0\end{pmatrix}$	$\begin{pmatrix}0&\sqrt{3}&0\end{pmatrix}$	$\begin{pmatrix}\sqrt{3}&0\end{pmatrix}$	$\begin{pmatrix}\sqrt{3}&0\end{pmatrix}$	
$\mathcal{F}_1$	$\begin{pmatrix}-\sqrt{2}&1\end{pmatrix}$	$\begin{pmatrix}-\sqrt{2}&1\end{pmatrix}$	$\begin{pmatrix}0&1&-1\\-1&-1&0\end{pmatrix}$	$\begin{pmatrix}\frac{1}{\sqrt{5}}&-\frac{4}{5}\end{pmatrix}$	$\begin{pmatrix}\sqrt{\frac{2}{7}}&-\frac{5}{7}\end{pmatrix}$	$\left(\frac{1}{5}\right)$
$\mathcal{F}_2$	$\begin{pmatrix}0&-\sqrt{2}\\-\sqrt{2}&-2\end{pmatrix}$	$\begin{pmatrix}0&-\sqrt{2}\\-\sqrt{2}&-2\end{pmatrix}$	$\begin{pmatrix}0&1&2\\1&0&-1\\2&-1&0\end{pmatrix}$	$\begin{pmatrix}0&\frac{1}{\sqrt{5}}\\\frac{1}{\sqrt{5}}&\frac{8}{5}\end{pmatrix}$	$\begin{pmatrix}0&\sqrt{\frac{2}{7}}\\\sqrt{\frac{2}{7}}&\frac{10}{7}\end{pmatrix}$	$\left(-\frac{2}{5}\right)$
$\mathcal{F}_3$	$\begin{pmatrix}0&-\sqrt{6}\end{pmatrix}$	$\begin{pmatrix}0&-\sqrt{6}\end{pmatrix}$	$\begin{pmatrix}\sqrt{3}&0&-\sqrt{3}\end{pmatrix}$	$\begin{pmatrix}0&\sqrt{\frac{3}{5}}\end{pmatrix}$	$\begin{pmatrix}0&\sqrt{\frac{6}{7}}\end{pmatrix}$	
$\mathcal{H}_1$	$\begin{pmatrix}0&0\\0&-3\end{pmatrix}$	$\begin{pmatrix}\frac{2}{3}&-\frac{2}{\sqrt{3}}\\-\frac{2}{\sqrt{3}}&-\frac{5}{3}\end{pmatrix}$	$\begin{pmatrix}0&0&0\\0&1&-2\\0&-2&-2\end{pmatrix}$	$\begin{pmatrix}-\frac{1}{3}&-\frac{2\sqrt{5}}{3}\\-\frac{2\sqrt{5}}{3}&-\frac{2}{3}\end{pmatrix}$	$\begin{pmatrix}-\frac{2}{3}&-\frac{2\sqrt{14}}{3}\\-\frac{2\sqrt{14}}{3}&-\frac{1}{3}\end{pmatrix}$	(1)
$\mathcal{H}_2$	(0)	(0)	$\begin{pmatrix}0&\sqrt{3}\end{pmatrix}$	$\begin{pmatrix}\sqrt{\frac{5}{3}}\end{pmatrix}$	$\begin{pmatrix}\sqrt{\frac{14}{3}}\end{pmatrix}$	(0)
$\mathcal{H}_3$	$\begin{pmatrix}0&0\end{pmatrix}$	$\begin{pmatrix}-\frac{2}{\sqrt{3}}&-\sqrt{\frac{2}{3}}\end{pmatrix}$	$\begin{pmatrix}0&-\sqrt{3}&-\sqrt{3}\end{pmatrix}$	$\begin{pmatrix}\frac{1}{\sqrt{3}}&-\sqrt{\frac{5}{3}}\end{pmatrix}$	$\begin{pmatrix}\frac{2}{\sqrt{3}}&-\sqrt{\frac{14}{3}}\end{pmatrix}$	

calculations, these corresponding operators in Eq. (A22) will be replaced by numerical matrices, which are summarized in Table VII.

[1] H. X. Chen, W. Chen, X. Liu, and S. L. Zhu, The hidden-charm pentaquark and tetraquark states, Phys. Rep. **639**, 1 (2016).

[2] X. Liu, An overview of XYZ new particles, Chin. Sci. Bull. **59**, 3815 (2014).

[3] R. Aaij *et al.* (LHCb Collaboration), Observation of J/ψ Resonances Consistent with Pentaquark States in $\Lambda_b^0 \to J/\psi K^- p$ Decays, Phys. Rev. Lett. **115**, 072001 (2015).

[4] R. Chen, X. Liu, X. Q. Li, and S. L. Zhu, Identifying Exotic Hidden-Charm Pentaquarks, Phys. Rev. Lett. **115**, 132002 (2015).

[5] H. X. Chen, W. Chen, X. Liu, T. G. Steele, and S. L. Zhu, Towards Exotic Hidden-Charm Pentaquarks in QCD, Phys. Rev. Lett. **115**, 172001 (2015).

[6] L. Roca, J. Nieves, and E. Oset, LHCb pentaquark as a $\bar{D}^*\Sigma_c - \bar{D}^*\Sigma_c^*$ molecular state, Phys. Rev. D **92**, 094003 (2015).

[7] J. He, $\bar{D}\Sigma_c^*$ and $\bar{D}^*\Sigma_c$ interactions and the LHCb hidden-charmed pentaquarks, Phys. Lett. B **753**, 547 (2016).

[8] T. J. Burns, Phenomenology of $P_c(4380)^+$, $P_c(4450)^+$ and related states, Eur. Phys. J. A **51**, 152 (2015).

[9] Y. Shimizu, D. Suenaga, and M. Harada, Coupled channel analysis of molecule picture of $P_c(4380)$, Phys. Rev. D **93**, 114003 (2016).

[10] R. Chen, X. Liu, and S. L. Zhu, Hidden-charm molecular pentaquarks and their charmed-strange partners, Nucl. Phys. **A954**, 406 (2016).

[11] H. Huang, C. Deng, J. Ping, and F. Wang, Possible pentaquarks with heavy quarks, Eur. Phys. J. C **76**, 624 (2016).

[12] H. X. Chen, E. L. Cui, W. Chen, X. Liu, T. G. Steele, and S. L. Zhu, QCD sum rule study of hidden-charm pentaquarks, Eur. Phys. J. C **76**, 572 (2016).

[13] G. Yang and J. Ping, The structure of pentaquarks P_c^+ in the chiral quark model, Phys. Rev. D **95**, 014010 (2017).

[14] J. He, Understanding spin parity of $P_c(4450)$ and $Y(4274)$ in a hadronic molecular state picture, Phys. Rev. D **95**, 074004 (2017).

[15] Y. Yamaguchi and E. Santopinto, Hidden-charm pentaquarks as a meson-baryon molecule with coupled channels for $\bar{D}^{(*)}\Lambda_c$ and $\bar{D}^{(*)}\Sigma_c^{(*)}$, Phys. Rev. D **96**, 014018 (2017).

[16] Y. Yamaguchi, A. Giachino, A. Hosaka, E. Santopinto, S. Takeuchi, and M. Takizawa, Hidden-charm and bottom meson-baryon molecules coupled with five-quark states, arXiv:1709.00819.

[17] C. J. Xiao and D. Y. Chen, Possible $B^{(*)}\bar{K}$ hadronic molecule state, Eur. Phys. J. A **53**, 127 (2017).

[18] S. S. Agaev, K. Azizi, and H. Sundu, Exploring $X(5568)$ as a meson molecule, Eur. Phys. J. Plus **131**, 351 (2016).

[19] T. J. Burns and E. S. Swanson, Interpreting the $X(5568)$, Phys. Lett. B **760**, 627 (2016).

[20] M. Albaladejo, J. Nieves, E. Oset, Z. F. Sun, and X. Liu, Can $X(5568)$ be described as a $B_s\pi$, $B\bar{K}$ resonant state?, Phys. Lett. B **757**, 515 (2016).

[21] R. Chen and X. Liu, Is the newly reported $X(5568)$ a $B\bar{K}$ molecular state?, Phys. Rev. D **94**, 034006 (2016).

[22] J. X. Lu, X. L. Ren, and L. S. Geng, $B_s\pi - B\bar{K}$ interactions in finite volume and $X(5568)$, Eur. Phys. J. C **77**, 94 (2017).

[23] B. X. Sun, F. Y. Dong, and J. L. Pang, Study of $X(5568)$ in a unitary coupled-channel approximation of $B\bar{K}$ and $B_s\pi$, Chin. Phys. C **41**, 074104 (2017).

[24] T. Barnes, F. E. Close, and H. J. Lipkin, Implications of a DK molecule at 2.32-GeV, Phys. Rev. D **68**, 054006 (2003).

[25] D. Zhang, Q. Y. Zhao, and Q. Y. Zhang, A Study of S-wave DK interactions in the chiral SU(3) quark model, Chin. Phys. Lett. **26**, 091201 (2009).

[26] F. K. Guo, P. N. Shen, H. C. Chiang, R. G. Ping, and B. S. Zou, Dynamically generated 0^+ heavy mesons in a heavy chiral unitary approach, Phys. Lett. B **641**, 278 (2006).

[27] Z. X. Xie, G. Q. Feng, and X. H. Guo, Analyzing $D_{s0}^*(2317)^+$ in the DK molecule picture in the Beth-Salpeter approach, Phys. Rev. D **81**, 036014 (2010).

[28] F. S. Navarra, M. Nielsen, E. Oset, and T. Sekihara, Testing the molecular nature of $D_{s0}^*(2317)$ and $D_0^*(2400)$ in semileptonic B_s and B decays, Phys. Rev. D **92**, 014031 (2015).

[29] F. K. Guo and U. G. Meissner, More kaonic bound states and a comprehensive interpretation of the D_{sJ} states, Phys. Rev. D **84**, 014013 (2011).

[30] F. K. Guo, P. N. Shen, and H. C. Chiang, Dynamically generated 1^+ heavy mesons, Phys. Lett. B **647**, 133 (2007).

[31] A. Faessler, T. Gutsche, V. E. Lyubovitskij, and Y. L. Ma, D^*K molecular structure of the $D_{s1}(2460)$ meson, Phys. Rev. D **76**, 114008 (2007).

[32] G. Q. Feng, X. H. Guo, and Z. H. Zhang, Studying the D^*K molecular structure of $D_s(2460)$ in the Bethe-Salpeter approach, Eur. Phys. J. C **72**, 2033 (2012).

[33] J. D. Weinstein and N. Isgur, Do Multi-Quark Hadrons Exist?, Phys. Rev. Lett. **48**, 659 (1982).

[34] J. D. Weinstein and N. Isgur, The $qq\ \bar{q}q$ system in a potential model, Phys. Rev. D **27**, 588 (1983).

[35] J. D. Weinstein and N. Isgur, $K\bar{K}$ molecules, Phys. Rev. D **41**, 2236 (1990).

[36] L. Roca, E. Oset, and J. Singh, Low lying axial-vector mesons as dynamically generated resonances, Phys. Rev. D **72**, 014002 (2005).

[37] F. Aceti, J. M. Dias, and E. Oset, $f_1(1285)$ decays into $a_0(980)\pi^0$, $f_0(980)\pi^0$ and isospin breaking, Eur. Phys. J. A **51**, 48 (2015).

[38] L. S. Geng, X. L. Ren, Y. Zhou, H. X. Chen, and E. Oset, S-wave KK^* interactions in a finite volume and the $f_1(1285)$, Phys. Rev. D **92**, 014029 (2015).

[39] P. L. Lü and J. He, Hadronic molecular states from the $K\bar{K}^*$ interaction, Eur. Phys. J. A **52**, 359 (2016).

[40] R. H. Dalitz and S. F. Tuan, A Possible Resonant State in Pion-Hyperon Scattering, Phys. Rev. Lett. **2**, 425 (1959).

[41] R. H. Dalitz and S. F. Tuan, The phenomenological description of K-nucleon reaction processes, Ann. Phys. (N.Y.) **10**, 307 (1960).

[42] T. Ezoe and A. Hosaka, Kaon-nucleon systems and their interactions in the Skyrme model, Phys. Rev. D **94**, 034022 (2016).

[43] R. Aaij *et al.* (LHCb Collaboration), Observation of Five New Narrow Ω_c^0 States Decaying to $\Xi_c^+K^-$, Phys. Rev. Lett. **118**, 182001 (2017).

[44] H. C. Kim, M. V. Polyakov, and M. Praszalowicz, Possibility of the existence of charmed exotica, Phys. Rev. D **96**, 014009 (2017); Publisher's Note, Phys. Rev. D **96**, 039902 (2017).

[45] G. Yang and J. Ping, The structure of pentaquarks Ω_c^0 in the chiral quark model, arXiv:1703.08845.

[46] H. Huang, J. Ping, and F. Wang, Investigating the excited Ω_c^0 states through Ξ_cK and $\Xi_c'K$ decay channels, arXiv:1704.01421.

[47] G. Montana, A. Feijoo, and A. Ramos, A meson-baryon molecular interpretation for some Ω_c excited baryons, arXiv:1709.08737.

[48] V. R. Debastiani, J. M. Dias, W. H. Liang, and E. Oset, Molecular Ω_c states within the local hidden gauge approach, arXiv:1710.04231.

[49] Y. R. Liu and M. Oka, Λ_cN bound states revisited, Phys. Rev. D **85**, 014015 (2012).

[50] Z.-w. Lin and C. M. Ko, A model for J/ψ absorption in hadronic matter, Phys. Rev. C **62**, 034903 (2000).

[51] H. Nagahiro, L. Roca, and E. Oset, Meson loops in the $f_0(980)$ and $a_0(980)$ radiative decays into ρ, ω, Eur. Phys. J. A **36**, 73 (2008).

[52] N. A. Tornqvist, From the deuteron to deusons, an analysis of deuteronlike meson-meson bound states, Z. Phys. C **61**, 525 (1994).

[53] N. A. Tornqvist, On deusons or deuteronlike meson-meson bound states, Nuovo Cimento Soc. Ital. Fis. **107A**, 2471 (1994).

[54] R. Chen, X. Liu, and A. Hosaka, Heavy molecules and one-σ/ω-exchange model, arXiv:1707.08306.

[55] E. Klempt, F. Bradamante, A. Martin, and J. M. Richard, Antinucleon-nucleon interaction at low energy: Scattering and protonium, Phys. Rep. **368**, 119 (2002).